mtDNA recombination indicative of hybridization suggests a role of the mitogenome in the adaptation of reef building corals to extreme environments

Eulalia Banguera-Hinestroza[1,2], Yvonne Sawall[3], Abdulmohsin Al-Sofyani[4], Patrick Mardulyn[2], Javier Fuertes-Aguilar[5], Heiber Cardenas-Henao[6], Francy Jimenez-Infante[1], Christian R. Voolstra[1**], Jean-François Flot [2**]*

1. Red Sea Research Center, King Abdullah University of Sciences and Technology (KAUST), Thuwal, Saudi Arabia.
2. Ecology and Evolutionary Biology, Université libre de Bruxelles (ULB), Brussels. Belgium.
3. Bermuda Institute of Ocean Sciences (BIOS), Coral Reef Ecology, Bermuda.
4. Department of Marine Biology, Faculty of Marine Sciences, King Abdulaziz University (KAU), Jeddah, Saudi Arabia.
5. Real Jardín Botánico, RJB-CSIC, Plaza de Murillo 2, 28014 Madrid, Spain.
6. Universidad del Valle, Department of Biology. Group of Ecogenetics and Molecular Biology, Cali, Colombia.

*Corresponding author: ebanguer@ulb.ac.be; eulalia.banguera@gmail.com

** Equal contributions

Abstract

Introgressive hybridization, as evidenced by topological incongruence between nuclear and mitochondrial phylogenies, has been broadly recorded in a range of organisms. However, mtDNA recombination following hybridization is rarely found in animals and was never until now reported in reef-building corals. Here we report unexpected topological incongruence among mitochondrial markers in the phylogenetic analysis of *Stylophora* species distributed along broad geographic ranges, including the full latitudinal (2000 km) and environmental gradient (21°C-33°C) of the Red Sea. The analysis of *Stylophora* lineages in the framework of the mitogenome phylogenies of members of the family Pocilloporidae, coupled with analyses of recombination, shows the first evidence of asymmetric patterns of introgressive hybridization associated to mitochondrial recombination in this genus. Hybridization likely occurred between an ancestral lineage restricted to the Red Sea/Gulf of Aden basins and migrants from the Indo-Pacific/Indian Ocean that reached the Gulf of Aden. The resulting hybrid occurs in sympatry with the parental Red Sea lineage, from which it inherited most of its mtDNA (except the recombinant region that includes the *nd6*, *atp6* and mt*ORF* genes) and expanded its range into the hottest region of the Arabian Gulf. Noticeably, across the Red Sea both lineages exhibit striking differences in terms of phylogenetic and phylogeographic patterns, clades-morphospecies association, and zooxanthellae composition. Our data suggest that the colonization of the Red Sea by the ancestral lineage, which involved overcoming the extreme temperatures of the southern Red Sea, likely resulted in changes in mitochondrial proteins, which led to its successful adaptation to the novel environmental conditions.

Key words: Introgressive hybridization, coral reefs, extreme environments, mtDNA recombination, mito-mito incongruence, mito-nuclear incongruence, *Stylophora*, Pocilloporidae, Red Sea.

1. INTRODUCTION

Studies of mitochondrial genomes have been of broad relevance for understanding the ecological and evolutionary processes leading to the diversification of organisms (Ballard and Rand, 2005; Chinnery and Hudson, 2013; Kivisild, 2015; Wolff et al., 2016), due particularly to key characteristics such as: maternal inheritance (in most organisms); high mutation rates in triploblastic metazoans (but not in cnidarians and poriferans; cf. Shearer et al. 2002); and lack of recombination (Barr et al., 2005). However, the latter assumption has been challenged by the increasing evidence of mtDNA recombination in animals (Barr et al., 2005; Ladoukakis and Zouros, 2017; Rokas et al., 2003; Tsaousis et al., 2005; Ujvari et al., 2007) with important ecological and evolutionary implications (Dokianakis and Ladoukakis, 2014; Levsen et al., 2016; Passamonti et al., 2013; Rokas et al., 2003; White et al., 2008).

In natural populations, most evidence for mtDNA and/or nuclear introgression comes from species living at the edge of their geographic range (i.e. marginal ecosystem that often exhibit genetically atypical populations; Johannesson and André, 2006), perturbed habitats, near extreme environmental conditions or in hybrid zones (Brennan et al., 2014; Hellberg et al., 2016; Johannesson and Carl, 2006; Riginos and Cunningham, 2004; Taylor et al., 2015). There is growing evidence in plants, in fungi, and to a lesser extent in animals, that divergent lineages that meet and interbreed in contact zones, particularly after expanding their range as a consequence of climatic or habitat fluctuations, produce hybrids carrying recombinant mitochondrial genomes (Barr et al., 2005) that are able to adapt to new environmental or habitat conditions leading eventually to hybrid speciation (Brennan et al., 2014; Mastrantonio et al., 2016; Riginos and Cunningham, 2004; Taylor et al., 2015).

Marginal areas such as the Red Sea, a biogeographic *cul-de-sac* extending from the Indian Ocean, are observed to host a high number of hybrid species (Berumen et al., 2017; DiBattista et al., 2016a; Garzón-Ospina et al., 2012; Johannesson and Carl, 2006; Veron, 1995) and therefore offer an interesting playground to study the main factors influencing patterns of diversification and hybrid speciation in extreme environments. The Red Sea ocean basin exhibits a high variability in oceanographic conditions following a N-S gradient along four well-defined oceanographic provinces (Raitsos et al., 2013), ranging from relatively low temperatures in the northern areas (below 23°C) to record summer temperatures up

to 33°C in the southern region (Acker et al., 2008; Moustafa et al., 2014; Raitsos et al., 2013; Sawall et al., 2015, 2014).

In addition, since its inception this region has undergone a complex climatic and geological history. During the last glacial cycles, the Red Sea experienced multiple sea-level fluctuations (Rohling et al., 2013; Siddall et al., 2003) as well as repetitive periods of connection and isolation from the Indo-Pacific, through the Strait of Bab-el-Mandeb in the South (Righton et al., 1996; Rohling et al., 2013; Siddall et al., 2004). These events, together with discontinuous periods of extinction and re-colonization from refuge zones inside and outside the region (Fine et al., 2013; Pellissier et al., 2014), likely played an important role in shaping the geographic distribution of genetic diversity for coral reefs in this oceanic basin, as well as the diversification of their associated fauna (Berumen et al., 2017; DiBattista et al., 2016a, 2016b, 2013). In fact, it has been postulated that corals entered the region during the Miocene –a period characterized by hyper-saline conditions and strong climate change – and after several episodes of post-Miocene migrations (Taviani, 1998). Lineages already inhabiting this area were affected by the successive geological and climatic processes influencing the region (DiBattista et al., 2016a). Repetitive invasions from the Indian Ocean likely enhanced the potential for the encounter of lineages with different genetic backgrounds, increasing the chance for hybridization and therefore hybrid speciation in the unique conditions of this marine zone.

Introgressive hybridization has been reported to be widespread in reef-building corals, with records mostly in the families Acroporidae, Poritidae and Pocilloporidae (Combosch and Vollmer, 2015; Forsman et al., 2017; Hellberg et al., 2016; Johnston et al., 2017; Richards and Hobbs, 2015; Van Oppen et al., 2001; Willis et al., 2006). Indeed, the topological incongruence observed in coral phylogenies might be explained by reticulate evolution due to multiple climatic and see-level changes across geological eras (Van Oppen et al., 2001; Veron, 1995; Vollmer and Palumbi, 2002; Willis et al., 2006). Moreover, it has been proposed that many species occurring in marginal areas and with restricted distribution, such as those endemic of the Indo-Pacific Ocean, might be hybrids (Richards and Hobbs, 2015; Veron, 1995). Even though mtDNA introgression is expected to be more frequent than nuclear introgression, particularly between species occurring in sympatry (Mastrantonio et al., 2016), it has not being reported to date in reef-building corals.

106 The coral genus *Stylophora* (family Pocilloporidae) is widely distributed in the Indo-Pacific and Indian
107 Ocean and comprises a range of a highly plastic morphospecies (Veron, 1995, 2002), which are
108 diversified within four phylogenetic lineages (Flot et al., 2011; Keshavmurthy et al., 2013; Stefani et al.,
109 2011). *Stylophora* is found throughout the entire environmental range of the Red Sea and is represented
110 by several morphospecies: *Stylophora pistillata* (Esper, 1797), *Stylophora subseriata* (Ehrenberg, 1834),
111 *Stylophora wellsi* (also found in Madagascar), *Stylophora kuelhmanni*, *Stylophora danae* and *Stylophora*
112 *mamillata* (Scheer and Pillai, 1983; Veron, 2002). A recent molecular study aiming to identify species
113 boundaries in the genus (Arrigoni et al., 2016) proposes that all these morphospecies belong to one
114 single cohesive molecular lineage.
115
116 Here, we studied the genetic variation of coral species within the genus *Stylophora* and their associated
117 zooxanthellae across the environmental gradients of the Red Sea, spanning over ~2000Km (12 degrees of
118 latitude), and included sequences from other relevant biogeographic regions (i.e. New Caledonia, Great
119 Barrier Reef, Madagascar, Gulf of Aden and Arabian Gulf). A total of 827 sequences were analyzed to
120 understand their genetic diversity, phylogenetic patterns and phylogeographic framework, in addition 281
121 colonies were typified for *Symbiodinium.* We selected this genus given its widespread geographical
122 distribution in the Indo-Pacific region and the presence of several endemic morphospecies in the Red Sea
123 (Veron et al., 2018), which may represent important sources of genetic variability for the future adaptation
124 of reef-building corals under the current threats of climate changes. Our molecular markers included ITS2
125 for *Symbiodinium* and four nuclear (*hsp70*, ITS1, ITS2 and *PMCA*) and five mitochondrial genes for the
126 coral host (mtCR, *cox1*, 12S, 16S and mt*ORF*). Among these markers, the hypervariable mt*ORF*, a
127 mitochondrial open reading frame of unknown function, which is unique to the family Pocilloporidae (Flot
128 and Tillier, 2007a), has been proposed as an alternative barcode for members of this family, performing
129 as well as NGS sequencing data for distinguishing species (i.e RAD-seq markers; Johnston et al., 2017).
130 But some authors such as Chen et al. (2008) considers the mt*ORF* as the control region, resulting in some
131 confusion in the literature.
132
133 Subsequently, the patterns of diversification of the Red Sea specimens were evaluated using full
134 mitochondrial genome sequences of species belonging to the family Pocilloporidae (*Pocillopora*,
135 *Seriatopora*, *Stylophora* and *Madracis*) (Veron and Pichon 1976). Our aims were (1) to investigate
136 patterns of diversification in *Stylophora* species and their associated zooxanthellae within the Red Sea and

verified further whether host morphological variation had any taxonomic value for these species (in other words, is there any association between morphological and genetic variation?). (2) to find out whether mitochondrial variation and phylogeographic patterns fit the trends expected from the environmental gradients in this marginal basin, and (3) to test whether the topological incongruence between mtDNA markers observed in our data and previously reported by Arrigoni et al. (2016) could be explained by introgressive hybridization. Here we discuss our results from an integrative perspective, coupling phylogenetic and phylogeographic patterns, *Symbiodinium* distribution, morphospecies-clades association and the finding of mtDNA recombination. We discuss the implications of these results for coral conservation in highly variable environments.

2. MATERIAL AND METHODS

2.1. Coral Sampling

We sampled a total of 725 colonies of *Stylophora* at 25 locations along the Red Sea coast in 2011 and 2012 from the Gulf of Aqaba in the North (Maqna, 28° 31' 34.20 N, 34° 48' 14.30" E) to Farasan Island in the South (16° 31' 38.5" N, 42° 01' 54.09" E). Our sampling design covered the entire environmental gradient (Temperature: ~21 in the north to ~33°C in the south; Salinity: 41 PSU in the north to 37 PSU in the south) of the Red Sea and the four oceanographic provinces as defined in Raitsos et al. (2013; Figure 1 and Supplementary Table *S1*). Colonies were determined to belong to morphotypes of *S. pistillata*, *S. subseriata*, *S. danae*, *S. kuelhmanni* and *S. wellsi* (Figure 1). Identification was carried out with the assistance of Dr. J.E.N Veron (personal communication) and by comparing his photographic records of Red Sea samples with our photographs taken during coral sampling. Small coral nubbins (~1cm) were collected in 3-7 m depth from colonies 5 m apart from each other to minimize sampling of clones and were preserved at room temperature in salt-saturated DMSO buffer (Gaither et al., 2011; Seutin et al., 1991)

2.2. DNA extraction, PCR and sequencing

Coral nubbins were placed in approximately 400 µL of lysis buffer (DNeasy Plant Minikit; Qiagen, Hilden, Germany®) with sterile glass beads and beaten for 30 s at full speed in a Qiagen Tissue Lyser II

(Qiagen, Hilden, Germany®). After cell lysis, DNA was extracted following the protocol recommended by the manufacturer. Five mitochondrial genes and four nuclear genes were amplified. First we barcoded our samples using the mt*ORF*, which is considered the most variable gene for Pocilloporidae (Flot and Tillier, 2007) and a short fragment of the adjacent ATPase subunit 6 gene (*atp6*). After this initial barcoding step, the mitochondrial control region (CR), the cytochrome *c* oxidase subunit I (*cox1*) and the mitochondrial 12S and 16S ribosomal RNA (rRNA) genes were amplified for a subset of samples. A subset was also amplified for several nuclear genes: the heat shock protein (*hsp70*) gene, the internal transcribed spacers (ITS1 and ITS2) and the Plasma Membrane Calcium ATPase (*PMCA*) gene. The 16S, 12S and *cox1* were amplified with primers designed in this study. The primers we included and their respective references are listed in the Supplementary Table *S2*.

After amplification, samples were cleaned using the Exostar 1-step protocol (Ilustra®) and sequenced in both forward and reverse directions; 5-10 specimens of each haplotype were sequenced twice to confirm the accuracy of the sequences. The forward and reverse chromatograms were assembled and edited using Chromas-Pro software version 2.1.5.1 (Technelysium, Pty Ltd). Sequences were first aligned using MUSCLE (Edgar, 2004) as implemented in MEGA version 7.0.26 (Kumar et al., 2016) and when the resulting alignment contained multiple gaps we used MAFFT's FFT-NS-i (Slow; iterative refinement method) to improve the alignment (Katoh and Standley, 2013). All alignments were confirmed and corrected by eye and sequences were trimmed to the same length for further analyses. For 12S and 16S, we removed a small region in which a long stretch of homopolymers did not allow high confidence in the alignment. Nuclear genes were phased using the programs PHASE Version 2.1 (Stephens and Donnelly, 2003) using the input files obtained in SeqPHASE (Flot, 2010).

In the few cases when ITS1, ITS2, or *PMCA* chromatograms showed multiple double peaks (as expected when sequencing a mixture of DNA sequences of unequal length; Flot et al., 2006) the indels from these chromatograms were not considered for downstream analyses and only clean regions with double peaks were included in the phasing process. In addition to our samples from the Red Sea, we amplified and sequenced the 12S and 16S markers of selected specimens from Flot et al. (2011) from several geographic regions (New Caledonia, Japan, Philippines and Madagascar). Moreover, previously published mt*ORF* and CR sequences (Flot et al., 2011; Stefani et al., 2011) as well as *hsp70* sequences (Klueter and Andreakis, 2013) from other geographic regions (i.e. Gulf of Aden and Indo-Pacific) as

well as from the Red Sea (i.e. mt*ORF* sequences belonging to *S. mamillata*: Arrigoni et al., 2016) were downloaded from the NCBI database and included in our analyses (accession numbers for these samples can be found in the respective references). Finally, we also included *cox1* sequences from Keshavmurthy et al. (2013) that were downloaded from the Dryad Digital Repository: (doi:10.5061/dryad.n2fb2).

2.3. Identification of zooxanthellae (*Symbiodinium*)

Symbiodinium types were identified by the amplification of the *ITS2* rDNA in a set of *Stylophora* samples from the Red Sea collected throughout the same gradient as described above (N=281). We used the DGGE-ITS2 protocol described in LaJeunesse (2002) with the primers and protocols recommended in LaJeunesse et al. (2003). DGGE gels, electrophoresis and PCR conditions are fully described in Arif et al. (2014). Sequences were processed using Chromas-Pro software version 1.7.5 (Technelysium, Pty Ltd) and phylogenetic assignments were built by comparisons with previously published *ITS2* sequences in the GeoSymbio data base (Franklin et al. 2012) and the Todd LaJeunesse's database (https://131.204.120.103/srsantos/symbiodinium/sd2_ged/database/views.php).

2.4. Sequence variation, phylogenetic and phylogeographic analyses

Number of haplotypes (h), polymorphic sites per gene, and shared haplotypes within and among Red Sea regions (Maqna, Al-Wajh, Yanbu, Kaust, Jeddah, Doga, Farasan, Gulf of Aden; Figure 1) as well as for other geographic locations (see above), were calculated using Arlequin version 3.5 (Excoffier and Lischer, 2010) and DNAsp version 5.1 (Librado and Rozas, 2009). Phylogenetic analyses were performed using *Stylophora* specimens from seven geographic regions (Caledonia, Japan, Philippines, Madagascar, Gulf of Aden, Arabian Gulf and Red Sea). When several sequences shared the same haplotype, a single representative was included in the data set for phylogenetic analyses.
To account for the phylogenetic signal in indels (insertion-deletion polymorphism) gaps were treated as missing data and coded as additional presence/absence (0-1) characters with the program Fastgap v1.2. (Borchsenius 2009) resulting in a data set with two data partitions: nucleotides and standard characters (0-1). This approach was used to infer Bayesian trees with a mixed model, which allows the combination of different data partitions with parameters unlinked across partitions (Huelsenbeck and Ronquist, 2001). The best evolutionary models for each gene and data partition were selected by

calculating their BIC (Bayesian Information Criterion) scores as recommended in MEGA v.7 (Kumar et al. 2016). The non-uniformity of evolutionary rates among sites was modelled using a discrete Gamma distribution (+G) with 5 rate categories and by assuming a portion of the sites to be invariant (+I). The gamma shape parameter, proportion of invariant sites, transition/transversion ratio, nucleotide frequencies and rates of substitutions were also estimated from the data.

Bayesian trees were built in MrBayes (Huelsenbeck and Ronquist, 2001) at the CIPRES Science Gateway v 3.1 (Miller et al., 2010). For each data set we performed 4 independent runs (nruns=4) with 1 cold and 3 heated chains (nchains=4). The total number of generations (ngen) was set at 10,000,000; sampling was performed every 1000 generations (Diagnfreq=1000); and the burn-in fraction was set to 25% (burninfrac=0.25). Convergence was assessed using the program Tracer v 1.7 (Rambaut and Drummond, 2009). Maximum Likelihood (ML) and Neighbor Joining (NJ trees) were built in MEGA v7 (Kumar et al., 2016), with 1000 bootstrap replicates, We used the nearest neighbor interchange algorithm (NNI) with an initial tree automatically generated (option: NJ/BioNJ) and the branch-swap filter set to strong, including all sites in the alignment. NJ trees were constructed using the Maximum Composite Likelihood method, with the pairwise deletion option activated. Trees were constructed for all markers, except 16S and *cox1* that showed little or no variability in *Stylophora* spp. (see results). mt*ORF* and CR phylogenies (using our complete data set) were built only using the alignable regions among all samples and the outgroups (*Pocillopora* and *Seriatopora*), and alternatively, excluding the outgroups to allow the analyses of longer fragments (in these cases, the root of the trees was placed in agreement with that inferred by the phylogeny using shorter fragments and by the loci in which the full outgroup sequences were included).

Relationships among haplotypes were explored for the three most variable markers (mt*ORF*, CR and *hsp70*) using the program HaplowebMaker (https://eeg-ebe.github.io/HaplowebMaker/; Spöri and Flot, in prep.) applying the median-joining algorithm. Haplotypes belonging to specimens from the Pacific regions and Madagascar were included, when possible, to identify patterns of colonization. The frequency of each haplotype along the environmental gradient of the Red Sea (i.e. each locality/population) was calculated using Arlequin v. 3.5 (Excoffier and Lischer, 2010).

2.5. Mitogenomes assembly and annotation

The complete mitogenomes of the two Red Sea lineages identify in our individual phylogenies analyses (see results) –called *RS_LinA* and *RS_LinB* hereafter– were obtained using two different approaches. First, paired-end Illumina reads from the draft genome of *Stylophora pistillata* (Voolstra et al. 2017) –identified as *RS_LinA*– were downloaded from the NCBI Short Read Archive (https://www.ncbi.nlm.nih.gov/sra/SRX999949) using fastq-dump (fastq-dump --origfmt --split-3 SRR1980974). Second, 1.7 Gb paired-end reads for the *RS_LinB* were obtained from Red Sea samples preserved in CHAOS buffer (Flot 2007) and extracted using the DNA NucleoSpin kit (Macherey-Nagel) following the protocol recommended by the company. Sequencing was performed in an Illumina NovaSeq 6000 at the BRIGHTcore facilities (Brussels Interuniversity Genomics High Throughput core)

The mitogenome of both lineages were assembled de novo from the raw Illumina reads using NOVOPlasty v2.7.1 (Dierckxsens et al., 2016) with the *cox1* gene as a seed. For the assembly of the *RS_LinB* mitogenome, both *cox1* and the complete mitogenome of the *RS_LinA* were used as seeds. Runs were performed without and with reference, using the mitogenome of *Stylophora pistillata* (NC_011162.1) for comparative purposes. The accuracy of the assembly was confirmed by mapping the reads back to the assembled genomes using Bowtie2. In addition, the identity of each lineage was corroborated by aligning the resulting genomes with sequences from six of the markers used for our interspecific phylogenies (mt*ORF*, CR, *atp6*, 12S, 16S and *cox1*). Genes were annotated using MITOS (Al Arab et al., 2017; Bernt et al., 2013). Alignment for each annotated gene was performed with MUSCLE (Edgar, 2004) and genes identities were confirmed using BLAST searches. When there was incongruence, particularly at the 5' and 3' ends of the genes, annotations were manually corrected using as reference standard (RefSeq) the mitogenome of *Stylophora pistillata* from the NCBI data base (NC_011162.1). Finally, genes were concatenated using Fastgap v1.2. (Borchsenius 2009) and aligned with mitogenomes from other members of the family Pocilloporidae using MAFFT (Katoh and Standley, 2013). The mitogenomes included were: *Seriatopora hystrix* (EF633600.2), *Seriatopora caliendrum* (EF633601.2), *Pocillopora damicornis* (EF526302.1; EU400213.1), *Pocillopora eydouxi* (EF526303.1), *Stylophora pistillata* (of Indo-Pacific origin; NC_011162.1) and *Madracis mirabilis* (EU400212.1).

2.6. Analyses of recombination and mitogenome phylogenies

Recombination was tested using the alignments of the full mitogenomes from members of the family Pocilloporidae, including the two divergent *Stylophora* lineages from the present study –see results –; the genus *Polyciathus* was also included as an external sequence. Seven heuristic recombination detection methods implemented in the RDP4 package (Martin et al., 2015) were used: RDP (Martin et al., 2010), BOOTSCAN (Martin et al., 2005), GENECONV (Padidam et al., 1999), MAXCHI (Maximum Chi Square method; Smith 1992); CHIMAERA (Posada and Crandall, 2001), SISCAN (Sister Scanning method; Gibbs et al. 2000), and 3SEQ (Boni et al., 2006).

The default settings were used for most methods, except for window sizes, step sizes and tree building methods. Window size was selected to include at least 10 variable nucleotide positions within every window examined. In RPD, SISCAN, and BOOTSCAN methods windows size were set at 100; in CHIMAERA and MAXCHI at 200. Alternatively, the MAXCHI and CHIMAERA methods were set to run with variable windows sizes, to allow the program to adjust the window size depending on degrees of parental sequence divergence as recommended by the author. Only recombination events detected with $P<0.05$, after Bonferroni correction were recorded.

The boundaries of the breakpoints were double checked by comparing the agreement of the boundaries between methods. The major parent and the minor parent hypothesized by the program, were contrasted against evidence from our phylogenetic and phylogeographic analyses. Furthermore, given that the parental ascription of the recombinant sequence may be difficult among closely related sequences, we refined the hypothesis by comparing the hypothesized distribution range of the major *Stylophora* clades (Keshavmurthy et al., 2013) and the supporting data from previous studies in hybrids species in the region and outside the Red Sea (DiBattista et al., 2015). It is important to note that the identified major and minor parents are not the "real" parental sequences, but sequences that are closely related to likely ancestral sequences, also that the recombinant region is related to the "minor" parent and the "non-recombinant" region related to the "major" parent (Martin et al., 2015).

Phylogenetic relationships among mitogenomes were inferred using maximum likelihood trees in PhylML (Guindon et al., 2010) available at the http://www.phylogeny.fr/index.cgi (Dereeper et al.,

2010, 2008). Branch support was evaluated using an Approximate Likelihood Ratio test (aLRT) (Anisimova and Gascuel, 2006). Trees were built for: (a) the full alignments, including and excluding the recombinant region and (b) genes within the recombinant region. The best model was selected as indicated in MEGA v7 (Kumar et al., 2016) as the GTR+G+I (General Time Reversible mode, non-uniformity of evolutionary rates among sites modeled using a discrete Gamma distribution with 5 rate categories and a fraction invariable sites). Because ambiguously aligned regions or highly divergent sequences can mislead recombination signals, we ran the analyses including and excluding the *mtORF* and the *atp8* gene, and also excluding ambiguously aligned regions within the mt*ORF*. Finally, to discard the influence of highly divergent sequences, we repeated the recombination analyses excluding the mitogenomes of *Madracis* and *Polyciatus* species. After analyses, polymorphic sites in hypervariable genes within the recombinant region for each *Stylophora* were calculated using DNAsp version 5.1 (Librado and Rozas, 2009).

3. RESULTS

3.1. Gene variation and polymorphic sites

Our largest data set consisted of 827 sequences of the mt*ORF* locus, which includes a short region of the adjacent *atp6* gene, from a large portion of the geographic distribution of *Stylophora* (Figure 1); it included 716 samples from our collection of the Red Sea, 3 samples from the Arabian Gulf, plus 108 sequences of *S. pistillata* morphospecies from Stefani et al. (2011) and Flot et al. (2011): from the Gulf of Aden (N=20), Pacific regions (N=60) and Madagascar (N=28). In addition, we produced a second dataset for four other mitochondrial fragments, from CR (N=401), *cox1* (N=147), 12S (N=72) and 16S (N=61) and four nuclear fragments, from *hsp70* (N=738), ITS1 (N=75), ITS2 (N=56) and *PMCA* (N=86) genes. This data set includes sequences from other studies (see material and methods section 2).

While the *atp6*-mt*ORF* locus (N=827; 884-943 bp) displayed a high level of polymorphism in *Stylophora* samples, the two *cox1* fragments (303-545 bp) were found monomorphic when comparing sequences across all Red Sea specimens. Pairwise comparisons among all individuals uncovered multiple synonymous and non-synonymous substitutions at the 5' end and 3' end of the mt*ORF* gene, but noticeably, the core region was composed mainly by duplicated tandem repeats, which were of

variable lengths and dissimilar among *Stylophora* specimens from the Red Sea (in terms of nucleotide composition and length of the repeat; data not shown). The CR (N=401; 757 bp) was the most variable of the non-coding markers, with polymorphism mainly caused by variation in the number of tandem repeats, some of them being specific to *Stylophora* specimens inhabiting different geographic areas. Polymorphic sites, indels and parsimony informative sites for mitochondrial and nuclear genes are recorded in Supplementary Table *S3*.

3.2. Phylogenetic analyses

ML and Bayesian phylogenies inferred from the *atp6*-mt*ORF* locus including *Pocillopora* as an outgroup (no shown) or excluding the outgroup (Figure 2a) showed a large phylogenetic subdivision between two groups, each associated with both high Bayesian Posterior Probabilities (BPP > 1.0) and high bootstrap values (> 99%). A first clade, (N=461; h=27) included some of the sequences from the Red Sea and the Gulf of Aden and those from the Arabian Gulf (N=373; h=12), plus sequences from Madagascar (N=28, h=6) and the Pacific (N=60; h=9); the second clade included the other specimens from the Red Sea and Gulf of Aden (N=366; h=14) –we refer to this clade as the Red Sea Lineage B (*RS_LinB*)– (Figure 2a). These two lineages were also evident in the mitogenome phylogenies of the family using the full *atp6* (678 bp) and *nd6* genes (564 bp) (Figure 3a) and in the phylogenies derived from our recombination analyses (Figure 3b) –See recombination results below–. In fact, the *atp6* gene revealed 50 and 45 polymorphic sites between *RS_LinB vs RS_LinA* and *RS_LinB* vs Indo-Pacific/Indian Ocean lineage respectively, and only 8 polymorphic sites between *RS_LinA* and the Indo-Pacific/Indian Ocean lineage.

In contrast, in the phylogenetic trees inferred from all other markers, whether mitochondrial (CR, 12S) or nuclear (ITS1; ITS2*, hsp70; PMCA*) (Figures 2b and Supplementary Figure *S1*), *RS_LinA* and *RS_LinB* sequences form a clade that exclude all sequences from Madagascar and from the Indo-Pacific region. There is therefore a major incongruence between the phylogenetic signal of *atp6*, *nd6* and the mt*ORF* vs the CR and 12S (Figure 2 and Figure 3a) and between mtDNA genes vs the nuclear genes. The ITS2 showed a pattern similar to that of the CR, in which *RS_LinA* and *RS_LinB* are almost completely separated; there is only one individual from *RS_LinB* placed inside the clade formed by

RS_LinA sequences, and vice versa, on the ITS2 tree (Supplementary Figure *S1*). The *cox1* and the 16S trees provided only little phylogenetic information (not shown).

3.3. Comparative analyses between *RS_LinA* and *RS_LinB*

3.3.1. Intraspecific phylogenies and morphospecies-clade association

Bayesian and ML trees obtained based on the full-length sequences of the *atp6*-mt*ORF* locus, thus analyzing members of each lineage (*RS_LinA,* 884 bp, h=33; *RS_LinB*, 943 bp, h=20) separately, are shown in Figure 4. In general, we found no clear association between Red Sea morphospecies and phylogenetic groups in the *RS_LinA* lineage. For example, some mitochondrial haplotypes were shared among different morphotypes or/and individuals exhibiting the same morphotypes were placed into different subclades (Figure 4a); the only exceptions were haplotypes belonging to morphotypes of *S. kuelhmanni*, that were all associated with subclade *LA1*, and those from *S. mamillata* –from Arrigoni et al. (2016)– that were exclusively found in subclade *LA3* (data not shown). Instead, in the *RS_LinB* lineage, morphotypes attributed to *S. subseriata* (called *Stylophora* cf. *subseriata* thereafter) were grouped in subclade *LB1* and displayed haplotypes found exclusively in the northern Red Sea –see phylogeographic analyses below– and were differentiated from morphotypes belonging to *S. pistillata* (mainly short and medium branched morphotypes, called as *Stylophora* cf. *pistillata* from now on), whose haplotypes were distributed mainly in the central-southern Red Sea and were placed in subclade *LB2* (Figure 4b).

3.3.2. *Symbiodinium* distribution

As for zooxanthellae, *Symbiodinium* type A1 (*Symbiodinium microadriaticum*) was the most abundant in members of *Stylophora* within the Red Sea (167 out of 281 colonies), followed by *Symbiodinium* type C160 (N=49). The distribution of these types was somehow different between members of each *Stylophora* mtDNA lineage (Figure 4). In colonies placed within the *RS_LinB* and inhabiting the northern Red Sea (i.e. subclade *LB1*; *Stylophora* cf. *subseriata*; N=76) the most abundant type was C160 (N=41) followed by type A1 (N=22) and few colonies presented both types (A1-C160; N=9). In contrast, colonies distributed in the central-southern areas (i.e. subclade *LB2*; i.e. *Stylophora* cf.

411 *pistillata*) were mainly associated with type A1 (40 out of 54 colonies) and the presence of C160 type,
412 or of this type in combination with A1 (A1-C160) were not detected. In southern regions, few colonies
413 exhibited the C1* type, which was not present in northern colonies and was always found in association
414 of type A1 (i.e. A1-C1*; N=10). Other C types or associations A1-C types were found in very low
415 abundance (i.e. in one colony). A high percentage of the colonies of the *Stylophora RS_LinA* (105
416 colonies out of 151) showed association with *Symbiodinium microadriaticum* in both northern and
417 southern regions. The few colonies carrying C160 or A1-C160 types were mainly found in Yanbu (7 out
418 of 11 colonies). The presence of C1* and A1-C1* types were detected mostly in colonies inhabiting the
419 southernmost area of the Red Sea (i.e. Farasan; 7 out of 8 colonies). Few C types (i.e. C161, C162,
420 C116) and combination of A1 with other types (i.e. A1-D, A1-C41, A1-B, A1-C1, A1-C19; A1-sp)
421 displayed low frequencies and some of them were exclusive of colonies belonging to this group (Figure
422 4).
423
424 **3.4. Comparative phylogeography of *RS_LinA* and *RS_LinB* and patterns of genetic variation**
425 **along the Red Sea gradient**
426
427 Median-joining networks were constructed for the markers for which we had the largest number of
428 sequences: *atp6*-mt*ORF* (N=827), CR (N=401) and *hsp70* (N=738). Each network indicates a clear
429 phylogeographic signal (i.e., there was a visible association between genetic variation and geographic
430 location). The north-south genetic differentiation was more pronounced for *RS_LinB* than for *RS_LinA*,
431 a pattern supported by all three loci (Figure 5). Haplotype frequencies along the gradient were somehow
432 different among lineages. In *RS_LinB* the highest frequencies of the most common haplotypes were
433 found either in northern or southern areas, while haplotype frequencies in *RS_LinA* showed a clinal
434 variation (Supplementary Figure *S2*). For the *hsp70*, haplotypes showed different frequencies along the
435 gradient when evaluated per mtDNA lineage (Supplementary Figure *S2c*) and the pattern was similar to
436 that shown by the *atp6*-mt*ORF* locus.
437
438 **3.5. mtDNA recombination analyses**
439
440 The analyses of the mitogenomes for all members of the family Pocilloporidae including *RS_LinA* and
441 *RS_LinB* and the genus *Polycyathus*, resulted in the detection of several recombination events in

pocilloporid corals. Recombination signals were detected in *Stylophora, Seriatopora and Madracis.* The signals for *Stylophora* and *Seriatopora* were confirmed when excluding the two divergent genomes of *Madracis* and *Polycyathus*. In *Stylophora* the strongest signal supported by all seven methods was found in *RS_LinA*, with the major parent hypothesized as the *RS_LinB* and the minor parent *Stylophora pistillata* (Taiwan). *P*-values were as follow: RDP = 1.175×10^{-10}; GENECONV = 8.96×10^{-11}; BOOTSCAN = 1.237×10^{-11}; MAXCHI = 7×10^{-16}; CHIMAERA = 4.019×10^{-03}; SISCAN = 1.090×10^{18} and 3SEQ = 2.969×10^{-29}. The boundaries of the breakpoints were placed at the end of the *nd2* genes by all methods, extending across the *nd6*, *atp6*, mt*ORF* and ending at the beginning of the *nd4* gene (Supplementary Figure *S3*). A second event, in which the recombinant region was transferred from *Pocillopora* to the *RS_LinB* was hypothesized, in this case the recombinant region was restricted to the *atp6* gene. A third event was detected, by only 3 methods, in *Seriatopora hystrix and Seriatopora caliendrum*.

Family phylogenies focused in *Stylophora* and including the region inherited from the minor parent (*S. pistillata*, Taiwan; 2415 bp) and the major parent (*RS_LinB*; 9555 bp) (Figure 3b) corroborated the phylogenetic patterns outlined for *RS_LinA* and *RS_LinB* in our interspecific phylogenies (Figure 2).

4. DISCUSSION

The results from our study show support for the hypothesis that mtDNA introgressive hybridization is the most likely cause of topological mito-mito incongruence in *Stylophora*. Our recombination analyses, using the full mitogenomes of pocilloporid corals (*Madracis, Pocillopora, Seriatopora* and *Stylophora*, including the two Red Sea lineages), provides evidence of mtDNA introgression in this group – particularly in *Stylophora*– strongly suggesting the existence of a hybrid lineage (*RS_LinA*) in the Red Sea, Gulf of Aden and Arabian Gulf. The mitogenome of this lineage contains introgressed genes from two divergent mitochondrial lineages: on mtDNA genes found in the recombinant region (i.e. covering the complete *nd6*, *atp6* and mt*ORF* genes), which have been inherited from a parental species included in a lineage distributed in the Indo-Pacific/Indian Ocean region, while all other mtDNA genes can be traced back to the ancestor of the *RS_LinB*. In the Red Sea, the *RS_LinA* is found in sympatric association with the descendants of its local parental species (*RS_LinB)*, and they harbour different phylogeographic patterns and different *Symbiodinium* composition. In addition, we found that

morphospecies placed within the *RS_LinB* agreed with phylogenetic subclades, which accounts for the presence of two divergent allopatric populations divided in northern and southern areas, consistent with environmental and oceanographic discontinuities, a trend that was completely absent in the hybrid *RS_LinA*.

The colonization of the extreme environments of Red Sea by the ancestral *RS_LinB* implied the development of adaptations to demanding temperature and salinity conditions. This likely involved selective pressures observed to multiple amino acid changes in mitochondrial proteins, evidenced by the highest substitution rate in the *atp6* and in the mt*ORF* genes of the *RS_LinB*, when compared with other *Stylophora* lineages, which suggest a role of such mtDNA genes in the adaptation to extreme environments. These results have important implications for the conservation of Red Sea species and corals.

4.1. Divergent mitochondrial lineages of *Stylophora* are present in the Red Sea

Our *atp6*-mt*ORF* phylogenetic analyses highlight the presence of two divergent sympatric *Stylophora* lineages in the Red Sea/Gulf of Aden/Arabian Gulf areas: the *RS_LinA* sharing a common ancestry with an Indo-Pacific/Indian Ocean/Madagascar lineage –placed in Clade 1– and the *RS_LinB* lineage, which form a unique clade on its own –Clade 2– (Figure 2). These lineages were also supported by the family phylogenies of the *atp6* and *nd6* genes (Figure 3a). Noticeably, these phylogenies showed topological incongruence with those of the CR/12S loci (Figures 2b, 2c). Furthermore, the four nuclear genes used in these analyses did not support the existence of *RS_LinA* and *RS_LinB* lineages (Supplementary Figure *S1*). The only nuclear gene that showed a similar phylogenetic pattern of that shown by the CR and 12S genes, was the ITS2, which likely imply that the ITS2, subject to concerted evolution, tells a similar evolutionary history to that of mitochondrial genes.

Mito-nuclear incongruence such as reported in this study have already been reported in the literature on many metazoans taxa (Forsman et al., 2017; Pavlova et al., 2013; Salvi et al., 2017; Toews and Brelsford, 2012; Willis et al., 2006) and they are frequently invoked as one of the main signatures of selection (Morales et al., 2015), the result of incomplete lineage sorting (DeBiasse et al., 2014; Richards and Hobbs, 2015; Van Oppen et al., 2001) or introgressive hybridization (Forsman et al., 2017b;

Gompert et al., 2008). The latter is often considered to be rampant in corals, with reticulate evolution having been proposed as one of the main processes that contributed, in great extent, to their successful adaptation after the geographical range expansions induced by several catastrophic events, such as the Cretaceous mass extinctions and the glacial events of the Plio-Pleistocene (Veron, 1995). Our finding of incongruity in the phylogenetic patterns among mitochondrial genes versus nuclear genes in *Stylophora*, are therefore consistent with multiples studies in reef building corals.

In addition, to our knowledge, the degree of incongruence in mtDNA genes found in our analyses has not being identified in others coral genera so far. In *Stylophora*, incongruence between the mt*ORF* and the *CR* topologies was reported by Arrigoni et al. (2016) and Stefani et al. (2011).These authors suggested that the most plausible hypothesis for explaining this finding was the presence of pseudogenes at the mitogenome of this group, but we found no evidence for stop codons or other signs of ORF disruption, rather evidence that this mt*ORF* may code for a functional transmembrane protein (Banguera-Hinestroza et al. unpublished results) as proposed by Flot and Tillier (2007). Therefore, we believe that other hypotheses such as recombination resulting from introgressive hybridization at the mtDNA genome of *Stylophora* are equally probable as the ones discussed in Stefani et al. (2011).

In species with a uniparental inheritance of mtDNA, genes are linked and are expected to show the same phylogenetic patterns (Ladoukakis and Zouros, 2017). However, contrasting topologies in mtDNA genes may arise as the result of mtDNA introgressive hybridization, which is known to have a clear impact in genealogical and phylogenetic reconstructions (White et al., 2008). The presence of divergent mitochondrial genomes in the germline of an organism (heteroplasmy) as the result of paternal leakage (Barr et al., 2005; Kuijper et al., 2015; Passamonti et al., 2013; Rokas et al., 2003) may result in mtDNA recombination (considering that heteroplasmy have remained without modifications in the oocyte cytoplasm long enough for allowing recombination between paternal and maternal mtDNA; White et al., 2008). In the case that the recombinant genome become fixed, viable, and passed to the following generations it would result in viable hybrids carrying a mixed mtDNA genome (Rokas et al., 2003; White et al., 2008; Wilton et al., 2018). Even though, heteroplasmy have not been recorded in reef-building corals, there is an increasing evidence that mtDNA recombination resulting from mtDNA introgressive hybridization is not rare in nature (Barr et al., 2005; Levsen et al., 2016; Piganeau et al., 2004; Rokas et al., 2003).

535 **4.2. mtDNA recombination explains topological incongruence**

536

537 Our recombination analyses hypothesized the *RS_LinA* as a recombinant sequence with high
538 probabilities in all methods (*P*-values ranging between 4.0 x 10^{-03} and 2.96 x 10^{-29}) with the major
539 parent being the sequence from *RS_LinB*, and only the minor parent the sequences from *S. pistillata*
540 from Taiwan. For *RS_LinA* the recombinant region –inherited from the minor parent –spans the full *nd6*,
541 *atp6* and mt*ORF* (Supplementary Figure *S3*), which explain that trees constructed with these genes
542 showed a common ancestry between the *RS_LinA* and the Indo-Pacific/Indian ocean/Madagascar
543 lineages, while the same trees show a strong diversification between these two lineages and the *RS_LinB*
544 (Figure 2 and Figure 3). Moreover, the *RS_LinA*, inherited most of its mtDNA genes from the ancestor
545 of *RS_LinB*. Therefore, it is expected that other mtDNA genes display a closest relationship between the
546 *RS_LinA* and the *RS_LinB*, as shown in our phylogenies for the CR and 12S genes and in the
547 mitogenome phylogenies excluding the recombinant region (Figure3b). Consequently, our data strongly
548 supports mtDNA introgressive hybridization followed by recombination as the main cause of mito-mito
549 topological incongruence in *Stylophora*.

550

551 We interpret these results as a strong evidence that *RS_LinA* likely arose from a hybridization event
552 between two ancestral *Stylophora* lineages. The introgression pattern follow that recorded in species of
553 hybrid zones, in which hybrids usually display an unequal mix of two mtDNA genetic backgrounds,
554 with most mitochondrial genes or genetic polymorphism passed from the genetic pool of the local
555 species to the genome of the "invader" species (asymmetric patterns of introgression; Harrison and
556 Larson, 2014).

557

558 **4.3. Interspecific phylogenies and comparative phylogeographic analyses**

559

560 As our study focuses at the population level –based on the three most variable genes used here: the
561 *hsp70*, the CR and the *mtORF* – markedly different phylogeographic patterns arises for *RS_LinA* and for
562 *RS_LinB* along the latitudinal and environmental gradient in the Red Sea (Figure 5). These patterns
563 show a strong structure for *RS_LinB*, in which the groups supported by the phylogenetic analyses
564 (Figure 4) have restricted distribution either in the northern Red Sea or in the southern Red Sea, with the
565 break between the two zones found around Yanbu, a trend that was supported by the distribution of the

haplotype frequencies along the gradient for each gene (Supplementary Figure *S2*). In contrast, a lack of association with northern and southern environmental provinces was found in members of *RS_LinA*, and rather a clinal variation in haplotype frequencies was found across the gradient (Supplementary Figure *S2*).

Both lineages were also remarkably different in terms of morphology and *Symbiodinium* association: in the northern Red Sea population of *RS_LinB* (i.e. subclade *LB1*; Figure 4b) most colonies were associated with morphotypes of *Stylophora subseriata* (as described in Veron et al. 2018) and *Symbiodinium* type C160; whereas the central-southern population (i.e. subclade LB2; Figure 4b) grouped mostly individuals described in the literature as *Stylophora pistillata* and were associated mainly with *Symbiodinium* type A1, but in contrast to the northern group, no colonies were found carrying C160 or A1-C160 *Symbiodinium* types. Contrary to the trends detected in *RS_LinB*, colonies belonging to the hybrid lineage (*RS_LinA*) showed high phenotypic plasticity and most colonies carried a *Symbiodinium* type A1 in both northern and southern regions (Figure 4).

The strong differences found in both lineages, in terms of phylogeography, population subdivision, and congruence/incongruence between morphology and phylogenies, reinforces the hypothesis of an early colonization of the Red Sea by members of *RS_LinB* and a recent colonization of *RS_LinA* in agreement with its hybrid origin. This evolutionary scenario could be explained on the light of the multiple processes that have affected the region during the last glacial periods, as well as of the demographic history of reef coral fauna in this region. Several studies targeting the geological dynamic of the Red Sea and the patterns of diversity and endemism of its fauna (DiBattista et al., 2016a, 2016b; Fine et al., 2013; Moustafa et al., 2014; Moustafa and Hallock, 2008; Rohling et al., 2008) indicate that early coral reefs inhabiting this region (i.e. likely present in the region since the Miocene; Taviani 1998) were able to survive extreme climatic variations in sea levels and periods of hyper salinity (Rohling et al., 2013; Siddall et al., 2003; Righton et al., 1996; Rohling et al., 2013) thanks to the presence of refuge areas in the northern Red Sea (i.e. the Gulf of Aqaba) and in the southern regions (i.e. Southern Red Sea and Gulf of Aden) (Fine et al., 2013; Moustafa et al., 2014; Pellissier et al., 2014). Therefore, isolation in these refuge zones leading to diversification and posterior recolonization may explain the differentiation in allopatry of northern and central-southern populations of *RS_LinB*.

Furthermore, the phylogeographic patterns, such as the one presented here are also in accordance with several biogeographic studies, showing that oceanographic conditions along the environmental gradient of the Red Sea (Raitsos et al., 2013; Sawall et al., 2015) have originated barriers to genetic flow, influenced strongly the population structure of several species, and shaped patterns of endemism in this region (DiBattista et al., 2016a; Nanninga et al., 2014; Saenz-Agudelo et al., 2015), despite the fact that they seem to have little impact on reef communities in terms of richness of species and species diversity (Roberts et al., 2016). For example, Nanninga et al. (2013) found a good correlation between the genetic differentiation among anemonefish (*Amphiprion bicinctus*) along the Saudi Arabian coast and the environmental heterogeneity in this basin, with the steadiest genetic break found at approximately 19°N (Southern Red Sea), which coincided with a sharp increase in turbidity in this zone. Results of our study also concur with those of Froukh and Kochzius (2008, 2007) who also found high genetic differentiation that were related to physical differences among fourline wrasse fish (*Larabicus quadrilineatus*) from the northern and southern Red Sea. On a larger scale, research on butterfly and angel fish by Roberts et al. (1992) and studies by DiBattista et al. (2013) have hypothesized that several reef fish species diversified and remained restricted to the Red Sea.

4.4. The diversification of *Stylophora* in the Red Sea and Gulf of Aden

Our phylogeographic analyses indicate a broad distribution of *RS_LinB* across the Red Sea but limited distribution in the Gulf of Aden (only few 5 out of 37 samples carrying a single mtDNA haplotypes were found in this region, see also Stephani et al. 2017) (Supplementary Figure *S2*), which suggest that the ancestor of *RS_LinB* was likely endemic of these regions, with the border of its distribution in the Gulf of Aden. This lineage likely interbred with a lineage of broader distribution in the Indo-Pacific/Indian-Ocean at the periphery of its range, which is also a confluence between several marine provinces: the Red Sea and Gulf of Aden, the western Indian Ocean, and Indo-Polynesian provinces, at zone that have been shown to hold several hybrid species (DiBattista et al., 2015). Moreover, the phylogenetic position of Arabian Gulf haplotypes, which were placed in the same subclades of the *RS_linA* specimens, implies that the hybrid expanded its range into the Arabian Gulf and into the Red Sea –where it lives in sympatry with the descendants of the parental lineage–

Our results concur with multiple studies that have identified a large number of hybrid species in the Red

627 Sea (Berumen et al., 2017; DiBattista et al., 2016a) and seem to fit in the model of hybrid zones and
628 marginal areas (Barton, 1979; Hewitt, 1988), in which species from a diverse range of taxonomic groups
629 (i.e. plants, yeasts and to a lesser extent animals) living at the edge of their geographic ranges produce
630 viable hybrids carrying recombinant mitogenomes (Barr et al., 2005; Rokas et al., 2003). These hybrids
631 are able to adapt to new climatic conditions, and diverge in sympatric association with their parental
632 species (Ballard and Whitlock, 2004; Barr et al., 2005; Fourie et al., 2018; Galtier, 2011; Leducq et al.,
633 2017; Mastrantonio et al., 2016; Peris et al., 2017; Rokas et al., 2003; Ujvari et al., 2007). Moreover, the
634 pattern found in our results in *Stylophora* were similar to those found in hybrid species of marine reef-
635 fishes, found at the intersection of three main biogeographical regions: the Red Sea and Gulf of Aden,
636 the western Indian Ocean and the Indo-Polynesian provinces (DiBattista et al., 2015). These authors
637 identify 14 hybrid species based in molecular markers and morphological characteristics, the gene flow
638 was unidirectional, and the parental species were found at the periphery of their distribution range,
639 where they showed the lowest abundance. Interestingly, as in our work with *Stylophora*, the reported
640 hybrids were found to be the result of intercrosses between endemic species, with restricted distribution
641 range in the Red Sea and Arabian Gulf, with species broadly distributed in the Indo-Pacific, and the
642 major parental species was at the limit of its distribution and almost absent from the Gulf of Aden area.
643
644 **4.5. Implications for conservation in a climate change scenario**
645
646 Under the current challenges that climatic change poses for coral reef ecosystems, particularly with the
647 rising of oceanic temperatures above the limit threshold of most species (1°C above mean summer
648 maximum) (Hughes et al., 2018; Pandolfi et al., 2011) evolutionary studies with a clear assessment of the
649 demographic history of species and populations are of great relevance, particularly to understand the main
650 mechanisms involved in adaptation and speciation in variable and extreme environments. Our study,
651 coupling recombination analyses, phylogenetic and phylogeographic patterns, suggest that mtDNA genes
652 may play a key role in adaptation to extreme environments in coral species.
653
654 Two genes, the *atp6* gene and the mt*ORF* gene showed high mutation rates and extreme variability in
655 the *RS_LinB* leading to amino acid and structural changes in their encoded proteins, particularly in the
656 mt*ORF* (Banguera-Hinestroza et al. unpublished data). Interestingly, the *atp6* gene is part of a group of
657 genes that are essential in releasing and controlling the proliferation of deleterious oxygen radicals

(ROS) in the mitochondria (Kühlbrandt., 2015; Wirth et al., 2016), which are known for causing oxidative damage to symbionts and corals during exposition to high temperatures, with the subsequent bleaching and dead of corals (Downs et al., 2002; Smith et al., 2005).

In *RS_LinB*, the frequencies of the most common haplotypes of the mt*ORF* locus were associated with coldest (north) or hottest (central-south) areas in the Red Sea (Supplementary Figure S2), a tendency that was also followed by the haplotype frequencies of the *hsp70* gene –a chaperone protein involved in heat stress response (Kvitt et al., 2016; Mayer and Bukau, 2005)–, suggesting that both proteins may have played a similar role in the adaptation to temperature in *RS_LinB* variants. This premise was supported by the computational characterization of the mt*ORF* protein (Banguera-Hinestroza et al. unpublished) in which searches against approx. 95 million protein domains classified in the CATH data base –using the pDomTHREADER approach (Lobley et al., 2009)–, revealed that domains in the mt*ORF* protein of *RS_LinB*, have the highest matches with annotated domains involved in the structural integrity of a complex or its assembly within or outside a cell (CATH domain code: 1s58A00) and domains that play a role in cell-to-cell, cell-to-matrix interactions, and response to stress (1ux6A01) with high levels of confidence ($0.001 < P < 0.01$).

These findings may suggest that selective pressures imposed by the extreme environmental variations in the Red Sea along multiple geological periods, may had have an impact in the mitogenome of this lineage, with consequences in adaptation and speciation, as have been found in other taxa evolving in a broad range of environmental conditions (Hill, 2017, 2016; Lamb et al., 2018). Even though the *RS_LinB* hybridized with an Indo-Pacific/Indian Ocean lineage, the resulting hybrid (*RS_LinA*) did not inherited the variation at the *nd6*, *atp6* and mt*ORF* genes, this open the question whether other mitochondrial genes or mtDNA mechanisms may play a role in hybrid speciation and adaptation, or whether the hybrid may be more vulnerable to strong temperature variation (i.e. nowadays the *RS_LinA* is very rare in the Arabian Gulf Area; Banguera-Hinestroza et al. unpublished results).

Taken together, our data indicate that hybridization in corals could be more complex than commonly expected, involving mechanisms such as mitochondrial metabolism and mitochondrial genome evolution as have been previoulsy emphasized by Dixon et al., (2015) that demonstrated a strong maternal effect in heat stress tolerance. Assisted hybridization has been proposed as an alternative for

conservation of coral reef via genetic rescue (Chan et al., 2018); however, little is known about the molecular mechanisms enhancing hybrid adaptation and speciation under extreme climatic conditions. A clear understanding of these mechanisms coupled with the demographic history of coral populations is therefore needed to pursue effective conservation plans.

Funding statement

This research was funded by King Abdullah University of Science and Technology (KAUST), Saudi Arabia (sample analysis) and by King Abdulaziz University (KAU) as part of the Jeddah Transect project (sample collection) and by a postdoctoral research fellowship from the Université libre de Bruxelles, Belgium.

Acknowledgments: The authors want to thank Dr. Veron for assistance with voucher identification, Dr. Saenz Agudelo for sample collections and recommendations, Dr. Bouwmeester for sample collection, Vanessa Robitzch for helping with the DNA extractions, Catalina Ramirez for her support in bioinformatics pipelines and Sebastien Santini - CNRS/AMU IGS UMR7256, for its effort in maintaining the excellence of the Phylogeny.fr site. We thanks to King Abdulaziz University (KAU) and the Bioscience Core Lab at KAUST for sharing their facilities.

5. REFERENCES

Acker, J., Leptoukh, G., Shen, S., Zhu, T., Kempler, S., 2008. Remotely-sensed chlorophylla observations of the northern Red Sea indicate seasonal variability and influence of coastal reefs. J. Mar. Syst. 69, 191–204. https://doi.org/10.1016/j.jmarsys.2005.12.006

Al Arab, M., Höner zu Siederdissen, C., Tout, K., Sahyoun, A.H., Stadler, P.F., Bernt, M., 2017. Accurate annotation of protein-coding genes in mitochondrial genomes. Mol. Phylogenet. Evol. 106, 209–216. https://doi.org/10.1016/j.ympev.2016.09.024

Anisimova, M., Gascuel, O., 2006. Approximate Likelihood-Ratio test for branches: A fast, accurate, and powerful alternative. Syst. Biol. 55, 539–552. https://doi.org/10.1080/10635150600755453

Arrigoni, R., Benzoni, F., Terraneo, T.I., Caragnano, A., Berumen, M.L., 2016. Recent origin and semi-permeable species boundaries in the scleractinian coral genus *Stylophora* from the Red Sea. Sci. Rep. 6, 34612. https://doi.org/10.1038/srep34612

720 Ballard, J.W.O., Rand, D.M., 2005. The population biology of mitochondrial DNA and its phylogenetic
721 implications. Annu. Rev. Ecol. Evol. Syst. 36, 621–642.
722 https://doi.org/10.1146/annurev.ecolsys.36.091704.175513
723 Ballard, J.W.O., Whitlock, M.C., 2004. The incomplete natural history of mitochondria. Mol. Ecol. 13,
724 729–744. https://doi.org/10.1046/j.1365-294X.2003.02063.x
725 Barr, C.M., Neiman, M., Taylor, D.R., 2005. Inheritance and recombination of mitochondrial genomes
726 in plants, fungi and animals. New Phytol. 168, 39–50. https://doi.org/10.1111/j.1469-
727 8137.2005.01492.x
728 Barton, N.H., 1979. The dynamics of hybrid zones. Heredity (Edinb). 43, 341–359.
729 https://doi.org/10.1038/hdy.1979.87
730 Bernt, M., Donath, A., Jühling, F., Externbrink, F., Florentz, C., Fritzsch, G., Pütz, J., Middendorf, M.,
731 Stadler, P.F., 2013. MITOS: Improved de novo metazoan mitochondrial genome annotation. Mol.
732 Phylogenet. Evol. 69, 313–319. https://doi.org/10.1016/j.ympev.2012.08.023
733 Berumen, M.L., DiBattista, J.D., Rocha, L.A., 2017. Introduction to virtual issue on Red Sea and
734 Western Indian Ocean biogeography. J. Biogeogr. 44, 1923–1926.
735 https://doi.org/10.1111/jbi.13036
736 Boni, M.F., Posada, D., Feldman, M.W., 2006. An exact nonparametric method for inferring mosaic
737 structure in sequence triplets. Genetics 176, 1035–1047.
738 https://doi.org/10.1534/genetics.106.068874
739 Brennan, A.C., Woodward, G., Seehausen, O., Muñoz-Fuentes, V., Moritz, C., Guelmami, A., Abbott,
740 R.J., Edelaar, P., 2014. Hybridization due to changing species distributions: Adding problems or
741 solutions to conservation of biodiversity during global change? Evol. Ecol. Res. 16, 475–491.
742 Chan, W.Y., Peplow, L.M., Menéndez, P., Hoffmann, A.A., van Oppen, M.J.H., 2018. Interspecific
743 hybridization may provide novel opportunities for coral reef restoration. Front. Mar. Sci. 5, 1–15.
744 https://doi.org/10.3389/fmars.2018.00160
745 Chen, C., Chiou, C.-Y., Dai, C.-F., Chen, C.A., 2008. Unique mitogenomic features in the scleractinian
746 family pocilloporidae (Scleractinia: Astrocoeniina). Mar. Biotechnol. 10, 538–553.
747 https://doi.org/10.1007/s10126-008-9093-x
748 Chinnery, P.F., Hudson, G., 2013. Mitochondrial genetics. Br. Med. Bull. 106, 135–159.
749 https://doi.org/10.1093/bmb/ldt017
750 Combosch, D.J., Vollmer, S. V, 2015. Trans-Pacific RAD-Seq population genomics confirms

introgressive hybridization in Eastern Pacific *Pocillopora* corals. Mol. Phylogenet. Evol. 88, 154–162. https://doi.org/10.1016/j.ympev.2015.03.022

DeBiasse, M.B., Nelson, B.J., Hellberg, M.E., 2014. Evaluating summary statistics used to test for incomplete lineage sorting: mito-nuclear discordance in the reef sponge *Callyspongia vaginalis*. Mol. Ecol. 23, 225–238. https://doi.org/10.1111/mec.12584

Dereeper, A., Audic, S., Claverie, J.M.M., Blanc, G., 2010. BLAST-EXPLORER helps you building datasets for phylogenetic analysis. BMC Evol. Biol. 10, 8. https://doi.org/10.1186/1471-2148-10-8

Dereeper, A., Guignon, V., Blanc, G., Audic, S., Buffet, S., Chevenet, F., Dufayard, J.F., Guindon, S., Lefort, V., Lescot, M., Claverie, J.M., Gascuel, O., 2008. Phylogeny.fr: robust phylogenetic analysis for the non-specialist. Nucleic Acids Res. 36, W465–W469. https://doi.org/10.1093/nar/gkn180

DiBattista, J.D., Berumen, M.L., Gaither, M.R., Rocha, L.A., Eble, J.A., Choat, J.H., Craig, M.T., Skillings, D.J., Bowen, B.W., 2013. After continents divide: comparative phylogeography of reef fishes from the Red Sea and Indian Ocean. J. Biogeogr. 40, 1170–1181. https://doi.org/10.1111/jbi.12068

DiBattista, J.D., Howard Choat, J., Gaither, M.R., Hobbs, J.P.A., Lozano-Cortés, D.F., Myers, R.F., Paulay, G., Rocha, L.A., Toonen, R.J., Westneat, M.W., Berumen, M.L., 2016a. On the origin of endemic species in the Red Sea. J. Biogeogr. 43, 13–30. https://doi.org/10.1111/jbi.12631

DiBattista, J.D., Roberts, M.B., Bouwmeester, J., Bowen, B.W., Coker, D.J., Lozano-Cortés, D.F., Howard Choat, J., Gaither, M.R., Hobbs, J.P.A., Khalil, M.T., Kochzius, M., Myers, R.F., Paulay, G., Robitzch, V.S.N., Saenz-Agudelo, P., Salas, E., Sinclair-Taylor, T.H., Toonen, R.J., Westneat, M.W., Williams, S.T., Berumen, M.L., 2016b. A review of contemporary patterns of endemism for shallow water reef fauna in the Red Sea. J. Biogeogr. 43, 423–439. https://doi.org/10.1111/jbi.12649

DiBattista, J.D., Rocha, L.A., Hobbs, J.-P.A., He, S., Priest, M.A., Sinclair-Taylor, T.H., Bowen, B.W., Berumen, M.L., 2015. When biogeographical provinces collide: hybridization of reef fishes at the crossroads of marine biogeographical provinces in the Arabian Sea. J. Biogeogr. 42, 1601–1614. https://doi.org/10.1111/jbi.12526

Diekmann, O. E., Bak, R. P. M., Stam, W. T., & Olsen, J. L. 2001. Molecular genetic evidence for probable reticulate speciation in the coral genus *Madracis* from a Caribbean fringing reef slope. Mar. Biol. 139, 221–233. https://doi.org/10.1007/s002270100584

782 Dierckxsens, N., Mardulyn, P., Smits, G., 2016. NOVOPlasty: de novo assembly of organelle genomes
783 from whole genome data. Nucleic Acids Res. 45, gkw955. https://doi.org/10.1093/nar/gkw955
784 Dixon, G.B., Davies, S.W., Aglyamova, G. V., Meyer, E., Bay, L.K., Matz, M. V., 2015. Genomic
785 determinants of coral heat tolerance across latitudes. Science. 348, 1460–1462.
786 https://doi.org/10.1126/science.1261224
787 Dokianakis, E., Ladoukakis, E.D., 2014. Different degree of paternal mtDNA leakage between male and
788 female progeny in interspecific *Drosophila* crosses. Ecol. Evol. 4, 2633–2641.
789 https://doi.org/10.1002/ece3.1069
790 Downs, C.A., Fauth, J.E., Halas, J.C., Dustan, P., Bemiss, J., Woodley, C.M., 2002. Oxidative stress and
791 seasonl coral bleaching. Free Radic. Biol. Med. 33, 533–543.
792 Edgar, R.C., 2004. MUSCLE: multiple sequence alignment with high accuracy and high throughput.
793 Nucleic Acids Research. 32, 1792–1797. https://doi.org/10.1093/nar/gkh340
794 Ehrenberg, C.G., 1834. Die Corallenthiere des Rothen Meeres physiologisch untersucht un systematisch
795 verzeichnet. gedruckt in der Druckerei der K. Akademie der Wissenschafte, Berlin (156)
796 Esper, E.J.C., 1797. Fortsetzungen der Pflanzenthiere in Abbildungen nach der Natur mit Farben
797 erleuchtet nebst Beschreibungen. Erster Theil. Raspische Buchhandlung, Nürnberg.
798 Excoffier, L., Lischer, H.E.L., 2010. Arlequin suite ver 3.5: A new series of programs to perform
799 population genetics analyses under Linux and Windows. Mol. Ecol. Resour. 10, 564–567.
800 https://doi.org/10.1111/j.1755-0998.2010.02847.x
801 Fine, M., Gildor, H., Genin, A., 2013. A coral reef refuge in the Red Sea. Glob. Chang. Biol. 19, 3640–
802 3647. https://doi.org/10.1111/gcb.12356
803 Flot, J.F., 2010. seqphase: a web tool for interconverting phase input/output files and fasta sequence
804 alignments. Mol. Ecol. Resour. 10, 162–166. https://doi.org/10.1111/j.1755-0998.2009.02732.x
805 Flot, J.F., Blanchot, J., Charpy, L., Cruaud, C., Licuanan, W.Y., Nakano, Y., Payri, C., Tillier, S., 2011.
806 Incongruence between morphotypes and genetically delimited species in the coral genus
807 *Stylophora*: phenotypic plasticity, morphological convergence, morphological stasis or interspecific
808 hybridization? BMC Ecol. 11, 22. https://doi.org/10.1186/1472-6785-11-22
809 Flot, J.F., Tillier, S., 2007. The mitochondrial genome of *Pocillopora* (Cnidaria: Scleractinia) contains
810 two variable regions: The putative D-loop and a novel ORF of unknown function. Gene 401, 80–
811 87. https://doi.org/10.1016/j.gene.2007.07.006
812 Flot J.F., 2007. Towards a molecular taxonomy of corals of the genus *Pocillopora*. Ph.D. thesis,

(Muséum national d'Histoire naturelle, Paris).

Flot, J.F., Tillier, A., Samadi, S., Tillier, S., 2006. Phase determination from direct sequencing of length-variable DNA regions. Mol. Ecol. Notes. https://doi.org/10.1111/j.1471-8286.2006.01355.x

Forsman, Z.H., Knapp, I.S.S., Tisthammer, K., Eaton, D.A.R., Belcaid, M., Toonen, R.J., 2017. Coral hybridization or phenotypic variation? Genomic data reveal gene flow between *Porites lobata* and *P. Compressa*. Mol. Phylogenet. Evol. 111, 132–148. https://doi.org/10.1016/j.ympev.2017.03.023

Fourie, G., Van der Merwe, N.A., Wingfield, B.D., Bogale, M., Wingfield, M.J., Steenkamp, E.T., 2018. Mitochondrial introgression and interspecies recombination in the *Fusarium fujikuroi* species complex. IMA Fungus 9, 37–63. https://doi.org/10.5598/imafungus.2018.09.01.04

Froukh, T., Kochzius, M., 2008. Species boundaries and evolutionary lineages in the blue green damselfishes *Chromis viridis* and *Chromis atripectoralis* (Pomacentridae). J. Fish Biol. 72, 451–457. https://doi.org/10.1111/j.1095-8649.2007.01746.x

Froukh, T., Kochzius, M., 2007. Genetic population structure of the endemic fourline wrasse (*Larabicus quadrilineatus*) suggests limited larval dispersal distances in the Red Sea. Mol. Ecol. 16, 1359–1367. https://doi.org/10.1111/j.1365-294X.2007.03236.x

Gaither, M.R., Szabó, Z., Crepeau, M.W., Bird, C.E., Toonen, R.J., 2011. Preservation of corals in salt-saturated DMSO buffer is superior to ethanol for PCR experiments. Coral Reefs 30, 329–333. https://doi.org/10.1007/s00338-010-0687-1

Galtier, N., 2011. The intriguing evolutionary dynamics of plant mitochondrial DNA. BMC Biol. 9, 61. https://doi.org/10.1186/1741-7007-9-61

Garzón-Ospina, D., López, C., Forero-Rodríguez, J., Patarroyo, M.A., 2012. Genetic Diversity and Selection in Three *Plasmodium vivax* Merozoite Surface Protein 7 (Pvmsp-7) Genes in a Colombian Population. PLoS One 7, e45962. https://doi.org/10.1371/journal.pone.0045962

Gibbs, M.J., Armstrong, J.S., Gibbs, A.J., 2000. Sister-Scanning: a Monte Carlo procedure for assessing signals in recombinant sequences. Bioinformatics 16, 573–582. https://doi.org/10.1093/bioinformatics/16.7.573

Gompert, Z., Forister, M.L., Fordyce, J.A., Nice, C.C., 2008. Widespread mito-nuclear discordance with evidence for introgressive hybridization and selective sweeps in Lycaeides. Mol. Ecol. 17, 5231–5244. https://doi.org/10.1111/j.1365-294X.2008.03988.x

Guindon, S., Dufayard, J.-F., Lefort, V., Anisimova, M., Hordijk, W., Gascuel, O., 2010. New algorithms and methods to estimate Maximum-Likelihood phylogenies: Asessing the performance

844 of PhyML 2.0. Syst. Biol. https://doi.org/10.1093/sysbio/syq010
845 Harrison, R.G., Larson, E.L., 2014. Hybridization, Introgression, and the nature of species boundaries. J.
846 Hered. 105, 795–809. https://doi.org/10.1093/jhered/esu033
847 Hellberg, M.E., Prada, C., Tan, M.H., Forsman, Z.H., Baums, I.B., 2016. Getting a grip at the edge:
848 recolonization and introgression in eastern Pacific *Porites* corals. J. Biogeogr. 43, 2147–2159.
849 https://doi.org/10.1111/jbi.12792
850 Hewitt, G.M., 1988. Hybrid zones-natural laboratories for evolutionary studies. Trends Ecol. Evol. 3,
851 158–167. https://doi.org/10.1016/0169-5347(88)90033-X
852 Hill, G.E., 2017. The mitonuclear compatibility species concept. Auk 134, 393–409.
853 https://doi.org/10.1642/AUK-16-201.1
854 Hill, G.E., 2016. Mitonuclear coevolution as the genesis of speciation and the mitochondrial DNA
855 barcode gap. Ecol. Evol. 6, 5831–5842. https://doi.org/10.1002/ece3.2338
856 Huelsenbeck, J.P., Ronquist, F., 2001. Mr. BAYES: Bayesian inference of phylogenetic trees.
857 Bioinformatics 17, 754–755. https://doi.org/10.1093/bioinformatics/17.8.754
858 Hughes, T.P., Kerry, J.T., Baird, A.H., Connolly, S.R., Dietzel, A., Eakin, C.M., Heron, S.F., Hoey,
859 A.S., Hoogenboom, M.O., Liu, G., McWilliam, M.J., Pears, R.J., Pratchett, M.S., Skirving, W.J.,
860 Stella, J.S., Torda, G., 2018. Global warming transforms coral reef assemblages. Nature 556, 492–
861 496. https://doi.org/10.1038/s41586-018-0041-2
862 Johannesson, K., Carl, A., 2006. Life on the margin: genetic isolation and diversity loss in a peripheral
863 marine ecosystem, the Baltic Sea. Mol. Ecol. 15, 2013–2029. https://doi.org/10.1111/j.1365-
864 294X.2006.02919.x
865 Johnston, E.C., Forsman, Z.H., Flot, J.-F., Schmidt-Roach, S., Pinzón, J.H., Knapp, I.S.S., Toonen, R.J.,
866 2017. A genomic glance through the fog of plasticity and diversification in *Pocillopora*. Sci. Rep.
867 7, 5991. https://doi.org/10.1038/s41598-017-06085-3
868 Katoh, K., Standley, D.M., 2013. MAFFT Multiple Sequence Alignment Software Version 7:
869 Improvements in Performance and Usability. Mol. Biol. Evol. 30, 772–780.
870 https://doi.org/10.1093/molbev/mst010
871 Keshavmurthy, S., Yang, S.-Y., Alamaru, A., Chuang, Y.-Y., Pichon, M., Obura, D., Fontana, S., De
872 Palmas, S., Stefani, F., Benzoni, F., MacDonald, A., Noreen, A.M.E., Chen, C., Wallace, C.C.,
873 Pillay, R.M., Denis, V., Amri, A.Y., Reimer, J.D., Mezaki, T., Sheppard, C., Loya, Y., Abelson, A.,
874 Mohammed, M.S., Baker, A.C., Mostafavi, P.G., Suharsono, B.A., Chen, C.A., 2013. DNA

875 barcoding reveals the coral “laboratory-rat”, *Stylophora pistillata* encompasses multiple identities.
876 Sci. Rep. 3, 1520. https://doi.org/10.1038/srep01520
877 Kivisild, T., 2015. Maternal ancestry and population history from whole mitochondrial genomes.
878 Investig. Genet. 6, 3. https://doi.org/10.1186/s13323-015-0022-2
879 Klueter, A., Andreakis, N., 2013. Assessing genetic diversity in the scleractinian coral *Stylophora*
880 *pistillata* (Esper 1797) from the Central Great Barrier Reef and the Coral Sea. Syst. Biodivers. 11,
881 67–76. https://doi.org/10.1080/14772000.2013.770419
882 Kühlbrandt, W., 2015. Structure and function of mitochondrial membrane protein complexes. BMC
883 Biol. 13, 89. https://doi.org/10.1186/s12915-015-0201-x
884 Kuijper, B., Lane, N., Pomiankowski, A., 2015. Can paternal leakage maintain sexually antagonistic
885 polymorphism in the cytoplasm? J. Evol. Biol. 28, 468–480. https://doi.org/10.1111/jeb.12582
886 Kumar, S., Stecher, G., Tamura, K., 2016. MEGA7: Molecular Evolutionary Genetics Analysis Version
887 7.0 for Bigger Datasets. Mol. Biol. Evol. 33, 1870–1874. https://doi.org/10.1093/molbev/msw054
888 Kvitt, H., Rosenfeld, H., Tchernov, D., 2016. The regulation of thermal stress induced apoptosis in
889 corals reveals high similarities in gene expression and function to higher animals. Sci. Rep. 6,
890 30359. https://doi.org/10.1038/srep30359
891 Ladoukakis, E.D., Zouros, E., 2017. Evolution and inheritance of animal mitochondrial DNA: Rules and
892 exceptions. J. Biol. Res. 24, 1–7. https://doi.org/10.1186/s40709-017-0060-4
893 Lamb, A.M., Gan, H.M., Greening, C., Joseph, L., Lee, Y.P., Morán-Ordóñez, A., Sunnucks, P.,
894 Pavlova, A., 2018. Climate-driven mitochondrial selection: A test in Australian songbirds. Mol.
895 Ecol. 27, 898–918. https://doi.org/10.1111/mec.14488
896 Leducq, J.-B., Henault, M., Charron, G., Nielly-Thibault, L., Terrat, Y., Fiumera, H.L., Shapiro, B.J.,
897 Landry, C.R., 2017. Mitochondrial recombination and introgression during speciation by
898 Hybridization. Mol. Biol. Evol. 34, 1947–1959. https://doi.org/10.1093/molbev/msx139
899 Levsen, N., Bergero, R., Charlesworth, D., Wolff, K., 2016. Frequent, geographically structured
900 heteroplasmy in the mitochondria of a flowering plant, ribwort plantain (*Plantago lanceolata*).
901 Heredity (Edinb). 117, 1–7. https://doi.org/10.1038/hdy.2016.15
902 Librado, P., Rozas, J., 2009. DnaSP v5: A software for comprehensive analysis of DNA polymorphism
903 data. Bioinformatics 25, 1451–1452. https://doi.org/10.1093/bioinformatics/btp187
904 Lobley, A., Sadowski, M.I., Jones, D.T., 2009. pGenTHREADER and pDomTHREADER: new
905 methods for improved protein fold recognition and superfamily discrimination. Bioinformatics 25,

1761–1767. https://doi.org/10.1093/bioinformatics/btp302

Martin, D.P., Lemey, P., Lott, M., Moulton, V., Posada, D., Lefeuvre, P., 2010. RDP3: A flexible and fast computer program for analyzing recombination. Bioinformatics 26, 2462–2463. https://doi.org/10.1093/bioinformatics/btq467

Martin, D.P., Murrell, B., Golden, M., Khoosal, A., Muhire, B., 2015. RDP4: Detection and analysis of recombination patterns in virus genomes. Virus Evol. 1, vev003. https://doi.org/10.1093/ve/vev003

Martin, D.P., Posada, D., Crandall, K.A., Williamson, C., 2005. A modified Bootscan algorithm for automated identification of recombinant sequences and recombination breakpoints. AIDS Res. Hum. Retroviruses 21, 98–102. https://doi.org/10.1089/aid.2005.21.98

Mastrantonio, V., Porretta, D., Urbanelli, S., Crasta, G., Nascetti, G., 2016. Dynamics of mtDNA introgression during species range expansion: insights from an experimental longitudinal study. Sci. Rep. 6, 30355. https://doi.org/10.1038/srep30355

Mayer, M.P., Bukau, B., 2005. Hsp70 chaperones: Cellular functions and molecular mechanism. Cell. Mol. Life Sci. 62, 670–684. https://doi.org/10.1007/s00018-004-4464-6

Miller, M.A., Pfeiffer, W., Schwartz, T., 2010. Creating the CIPRES Science Gateway for inference of large phylogenetic trees, in: 2010 Gateway Computing Environments Workshop (GCE). IEEE, pp. 1–8. https://doi.org/10.1109/GCE.2010.5676129

Morales, H.E., Pavlova, A., Joseph, L., Sunnucks, P., 2015. Positive and purifying selection in mitochondrial genomes of a bird with mitonuclear discordance. Mol. Ecol. 24, 2820–37. https://doi.org/10.1111/mec.13203

Moustafa, M.Z., Hallock, P., 2008. Observations of a Red Sea Fringing Coral Reef under Extreme Environmental Conditions. 11th Int. Coral Reef Symp. Ft. Lauderdale, Florida 7–11.

Moustafa, M.Z., Moustafa, M.S., Moustafa, Z.D., Moustafa, S.E., 2014. Survival of high latitude fringing corals in extreme temperatures: Red Sea oceanography. J. Sea Res. 88, 144–151. https://doi.org/10.1016/j.seares.2014.01.012

Nanninga, G.B., Saenz-Agudelo, P., Manica, A., Berumen, M.L., 2014. Environmental gradients predict the genetic population structure of a coral reef fish in the Red Sea. Mol. Ecol. 23, 591–602. https://doi.org/10.1111/mec.12623

Padidam, M., Sawyer, S., Fauquet, C.M., 1999. Possible emergence of new gemini viruses by frequent recombination. Virology 265, 218–225. https://doi.org/10.1006/viro.1999.0056

Pandolfi, J.M., Connolly, S.R., Marshall, D.J., Cohen, A.L., 2011. Projecting coral reef futures under

937 global warming and ocean acidification. Science. 333, 418–422.
938 https://doi.org/10.1126/science.1204794
939 Passamonti, M., Ghiselli, F., Milani, L., 2013. Mitochondrial Inheritance, in: Brenner's Encyclopedia of
940 Genetics. Elsevier, pp. 443–445. https://doi.org/10.1016/B978-0-12-374984-0.00960-8
941 Pavlova, A., Amos, J.N., Joseph, L., Loynes, K., Austin, J.J., Keogh, J.S., Stone, G.N., Nicholls, J.A.,
942 Sunnucks, P., 2013. Perched at the mito-nuclear crossroads: divergent mitochondrial lineages
943 correlate with environment in the face of ongoing nuclear gene flow in an australian bird.
944 Evolution. 67, 3412–3428. https://doi.org/10.1111/evo.12107
945 Pellissier, L., Leprieur, F., Parravicini, V., Cowman, P.F., Kulbicki, M., Litsios, G., Olsen, S.M., Wisz,
946 M.S., Bellwood, D.R., Mouillot, D., 2014. Quaternary coral reef refugia preserved fish diversity.
947 Science. 344, 1016–1019. https://doi.org/10.1126/science.1249853
948 Peris, D., Arias, A., Orlić, S., Belloch, C., Pérez-Través, L., Querol, A., Barrio, E., 2017. Mitochondrial
949 introgression suggests extensive ancestral hybridization events among *Saccharomyces* species.
950 Mol. Phylogenet. Evol. 108, 49–60. https://doi.org/10.1016/j.ympev.2017.02.008
951 Piganeau, G., Gardner, M., Eyre-Walker, A., 2004. A broad survey of recombination in animal
952 mitochondria. Mol. Biol. Evol. https://doi.org/10.1093/molbev/msh244
953 Posada, D., Crandall, K.A., 2001. Evaluation of methods for detecting recombination from DNA
954 sequences: Computer simulations. Proc. Natl. Acad. Sci. 98, 13757–13762.
955 https://doi.org/10.1073/pnas.241370698
956 Raitsos, D.E., Pradhan, Y., Brewin, R.J.W., Stenchikov, G., Hoteit, I., 2013. Remote Sensing the
957 Phytoplankton Seasonal Succession of the Red Sea. PLoS One 8, e64909.
958 https://doi.org/10.1371/journal.pone.0064909
959 Rambaut, A., Drummond, A.J., 2009. Tracer v 1.5. http://beast.bio.ed.ac.uk/Tracer.
960 Richards, Z.T., Hobbs, J.P.A., 2015. Hybridisation on coral reefs and the conservation of evolutionary
961 novelty. Curr. Zool. 61, 132–145. https://doi.org/10.1093/czoolo/61.1.132
962 Righton, D., Kemp, J., Ormond, R., 1996. Biogeography community structure and diversity of Red Sea
963 and western Indian Ocean butterflyfishes. J. Mar. Biol. Assoc. United Kingdom 76, 223–228.
964 Riginos, C., Cunningham, C.W., 2004. Invited Review: Local adaptation and species segregation in two
965 mussel (*Mytilus edulis* × *Mytilus trossulus*) hybrid zones. Mol. Ecol. 14, 381–400.
966 https://doi.org/10.1111/j.1365-294X.2004.02379.x
967 Roberts, M.B., Jones, G.P., McCormick, M.I., Munday, P.L., Neale, S., Thorrold, S., Robitzch, V.S.N.,

968 Berumen, M.L., 2016. Homogeneity of coral reef communities across 8 degrees of latitude in the
969 Saudi Arabian Red Sea. Mar. Pollut. Bull. 105, 558–565.
970 https://doi.org/10.1016/j.marpolbul.2015.11.024
971 Rohling, E.J., Grant, K., Hemleben, C., Siddall, M., Hoogakker, B.A.A., Bolshaw, M., Kucera, M.,
972 2008. High rates of sea-level rise during the last interglacial period. Nat. Geosci. 1, 38–42.
973 https://doi.org/10.1038/ngeo.2007.28
974 Rohling, E.J., Grant, K.M., Roberts, A.P., Larrasoaña, J.-C., 2013. Paleoclimate variability in the
975 mediterranean and red sea regions during the last 500,000 years. Curr. Anthropol. 54, S183–S201.
976 https://doi.org/10.1086/673882
977 Rokas, A., Ladoukakis, E., Zouros, E., 2003. Animal mitochondrial DNA recombination revisited.
978 Trends Ecol. Evol. 18, 411–417. https://doi.org/10.1016/S0169-5347(03)00125-3
979 Saenz-Agudelo, P., Dibattista, J.D., Piatek, M.J., Gaither, M.R., Harrison, H.B., Nanninga, G.B.,
980 Berumen, M.L., 2015. Seascape genetics along environmental gradients in the Arabian Peninsula:
981 insights from ddRAD sequencing of anemonefishes. Mol. Ecol. 24, 6241–6255.
982 https://doi.org/10.1111/mec.13471
983 Salvi, D., Pinho, C., Harris, D.J., 2017. Digging up the roots of an insular hotspot of genetic diversity:
984 Decoupled mito-nuclear histories in the evolution of the Corsican-Sardinian endemic lizard
985 *Podarcis tiliguerta*. BMC Evol. Biol. 17. https://doi.org/10.1186/s12862-017-0899-x
986 Sawall, Y., Al-Sofyani, A., Banguera-Hinestroza, E., Voolstra, C.R., 2014. Spatio-temporal analyses of
987 *symbiodinium* physiology of the coral *Pocillopora verrucosa* along large-scale nutrient and
988 temperature gradients in the Red Sea. PLoS One 9, e103179.
989 https://doi.org/10.1371/journal.pone.0103179
990 Sawall, Y., Al-Sofyani, A., Hohn, S., Banguera-Hinestroza, E., Voolstra, C.R., Wahl, M., 2015.
991 Extensive phenotypic plasticity of a Red Sea coral over a strong latitudinal temperature gradient
992 suggests limited acclimatization potential to warming. Sci. Rep. 5, 8940.
993 https://doi.org/10.1038/srep08940
994 Scheer, G., Pillai, C.S.G., 1983. Report on the stony corals from the Red Sea. Zoologica 131, 1–198.
995 Seutin, G., White, B.N., Boag, P.., 1991. Preservation of avian blood and tissue samples for DNA
996 analyses. Can. J. Zool. 69, 89–90.
997 Shearer, T.L., Oppen, M.J.H. Van, Romano, S.L., G. Worheire, 2002. Slow mitochondria DNA
998 sequence evolution in the Anthozoa. Mol. Ecol. 11, 2475–2487.

999 Siddall, M., Rohling, E.J., Almogi-Labin, A., Hemleben, C., Meischner, D., Schmelzer, I., Smeed, D. a,
1000 2003. Sea-level fluctuations during the last glacial cycle. Nature 423, 853–858.
1001 https://doi.org/10.1038/nature01690
1002 Siddall, M., Smeed, D.A., Hemleben, C., Rohling, E.J., Schmelzer, I., Peltier, W.R., 2004.
1003 Understanding the Red Sea response to sea level. Earth Planet. Sci. Lett. 225, 421–434.
1004 https://doi.org/DOI 10.1016/j.epsl.2004.06.008
1005 Smith, D.J., Suggett, D.J., Baker, N.R., 2005. Is photoinhibition of zooxanthellae photosynthesis the
1006 primary cause of thermal bleaching in corals? Glob. Chang. Biol. 11, 1–11.
1007 https://doi.org/10.1111/j.1529-8817.2003.00895.x
1008 Smith, J., 1992. Analyzing the mosaic structure of genes. J. Mol. Evol. 34.
1009 https://doi.org/10.1007/BF00182389
1010 Stefani, F., Benzoni, F., Yang, S.-Y., Pichon, M., Galli, P., Chen, C.A., 2011. Comparison of
1011 morphological and genetic analyses reveals cryptic divergence and morphological plasticity in
1012 *Stylophora* (Cnidaria, Scleractinia). Coral Reefs 30, 1033–1049. https://doi.org/10.1007/s00338-
1013 011-0797-4
1014 Stephens, M., Donnelly, P., 2003. A Comparison of bayesian methods for haplotype reconstruction from
1015 population genotype data. Am. J. Hum. Genet. 73, 1162–1169. https://doi.org/10.1086/379378
1016 Taviani, M., 1998. Post-Miocene reef faunas of the Red Sea: glacio-eustatic controls, in: Sedimentation
1017 and tectonics in rift basins Red Sea-Gulf of Aden. Springer Netherlands, Dordrecht, pp. 574–582.
1018 https://doi.org/10.1007/978-94-011-4930-3_30
1019 Taylor, S.A., Larson, E.L., Harrison, R.G., 2015. Hybrid zones: windows on climate change. Trends
1020 Ecol. Evol. 30, 398–406. https://doi.org/10.1016/j.tree.2015.04.010
1021 Toews, David P.L. Brelsford, A., 2012. The biogeography of mitochondrial and nuclear discordance in
1022 animals. Mol. Ecol. 21, 3907–3930. https://doi.org/10.1111/j.1365-294X.2012.05664.x
1023 Tsaousis, A.D., Martin, D.P., Ladoukakis, E.D., Posada, D., Zouros, E., 2005. Widespread
1024 recombination in published animal mtDNA sequences. Mol. Biol. Evol. 22, 925–933.
1025 https://doi.org/10.1093/molbev/msi084
1026 Ujvari, B., Dowton, M., Madsen, T., 2007. Mitochondrial DNA recombination in a free-ranging
1027 Australian lizard. Biol. Lett. 3, 189–192. https://doi.org/10.1098/rsbl.2006.0587
1028 Van Oppen, M.J.H., McDonald, B.J., Willis, B., Miller, D.J., 2001. The evolutionary history of the coral
1029 genus *Acropora* (Scleractinia, Cnidaria) based on a mitochondrial and a nuclear marker:

1030 reticulation, incomplete lineage sorting, or morphological convergence? Mol. Biol. Evol. 18, 1315–
1031 1329. https://doi.org/11420370
1032 Veron, J.E.., 1995. J. E. N. Veron, 1995. Corals in space and time: the biogeography and evolution of
1033 the Scleractinia. Cornell Univ. Press. https://doi.org/10.1017/S0016756800008050
1034 Veron, J.E.. E.N., 2002. New Species Described in Corals of the World. Science. 11, 205.
1035 Vollmer, S. V., Palumbi, S.R., 2002. Hybridization and the evolution of reef coral diversity. Science.
1036 296, 2023–2025. https://doi.org/10.1126/science.1069524
1037 White, D.J., Wolff, J.N., Pierson, M., Gemmell, N.J., 2008. Revealing the hidden complexities of
1038 mtDNA inheritance. Mol. Ecol. 17, 4925–42. https://doi.org/10.1111/j.1365-294X.2008.03982.x
1039 Willis, B.L., van Oppen, M.J.H., Miller, D.J., Vollmer, S. V., Ayre, D.J., 2006. The role of hybridization
1040 in the evolution of reef corals. Annu. Rev. Ecol. Evol. Syst. 37, 489–517.
1041 https://doi.org/10.1146/annurev.ecolsys.37.091305.110136
1042 Wilton, P.R., Zaidi, A., Makova, K., Nielsen, R., 2018. A population phylogenetic view of
1043 mitochondrial heteroplasmy. Genetics 208, 1261–1274.
1044 https://doi.org/10.1534/genetics.118.300711
1045 Wirth, C., Brandt, U., Hunte, C., Zickermann, V., 2016. Structure and function of mitochondrial
1046 complex I. Biochim. Biophys. Acta - Bioenerg. 1857, 902–914.
1047 https://doi.org/10.1016/j.bbabio.2016.02.013
1048 Wolff, J.N., Pichaud, N., Camus, M.F., Côté, G., Blier, P.U., Dowling, D.K., 2016. Evolutionary
1049 implications of mitochondrial genetic variation: mitochondrial genetic effects on OXPHOS
1050 respiration and mitochondrial quantity change with age and sex in fruit flies. J. Evol. Biol. 29, 736–
1051 747. https://doi.org/10.1111/jeb.12822

Figure 1.

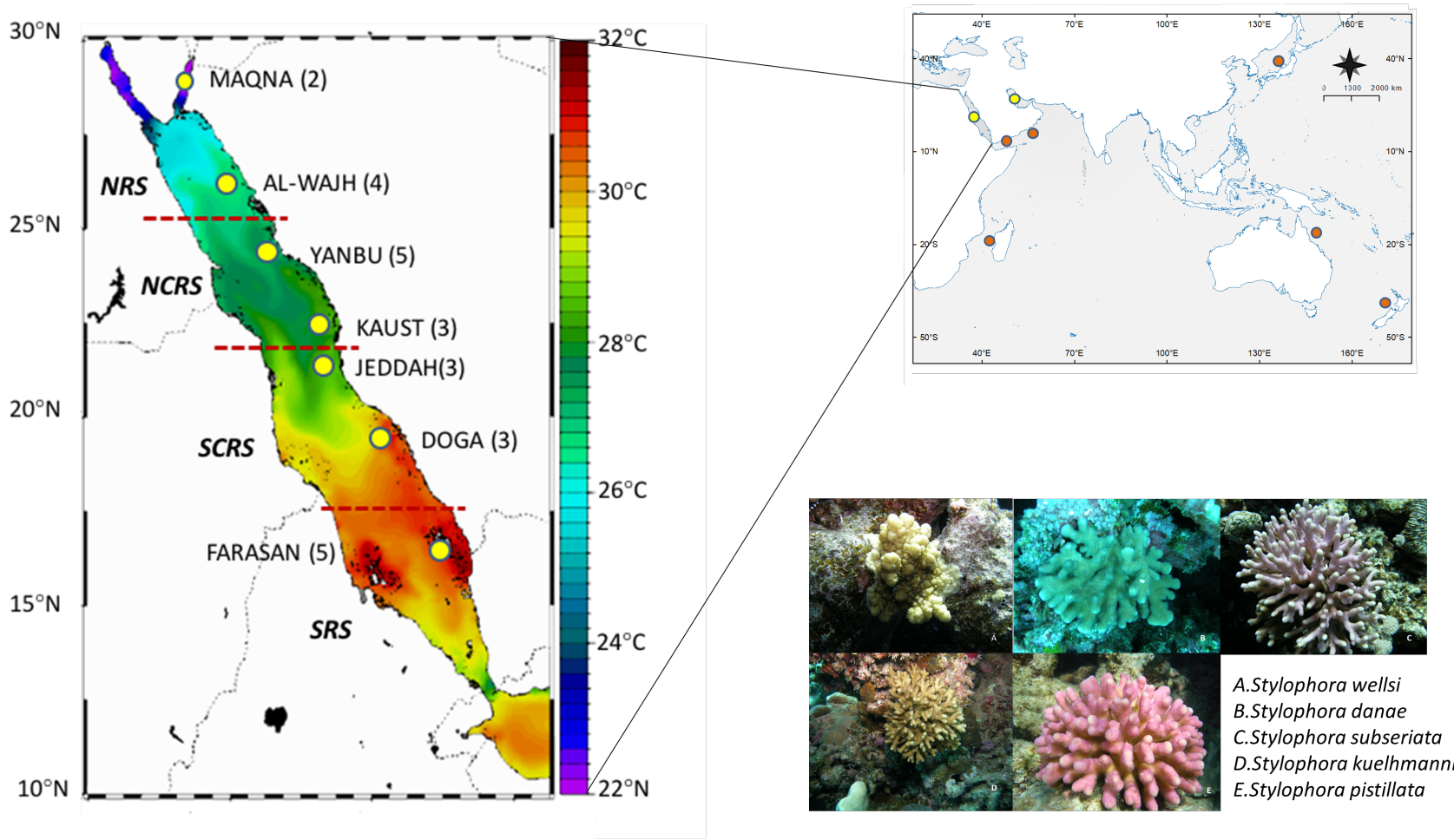

Sampling sites and *Stylophora* morphotypes collected in this study. Red Lines are indicating the barriers in oceanographic provinces described by Raitsos et al., (2013). Yellow points are sampling localities visited during this study. Reefs sampled in each location are included in parenthesis. Red points are sequences from other studies. The map was modified from the original downloaded from https://www7320.nrlssc.navy.mil/global_ncom/glb8_3b/html/Links/red/temp_glb8_3b_2012060700_0000m.gif

Figure 2.

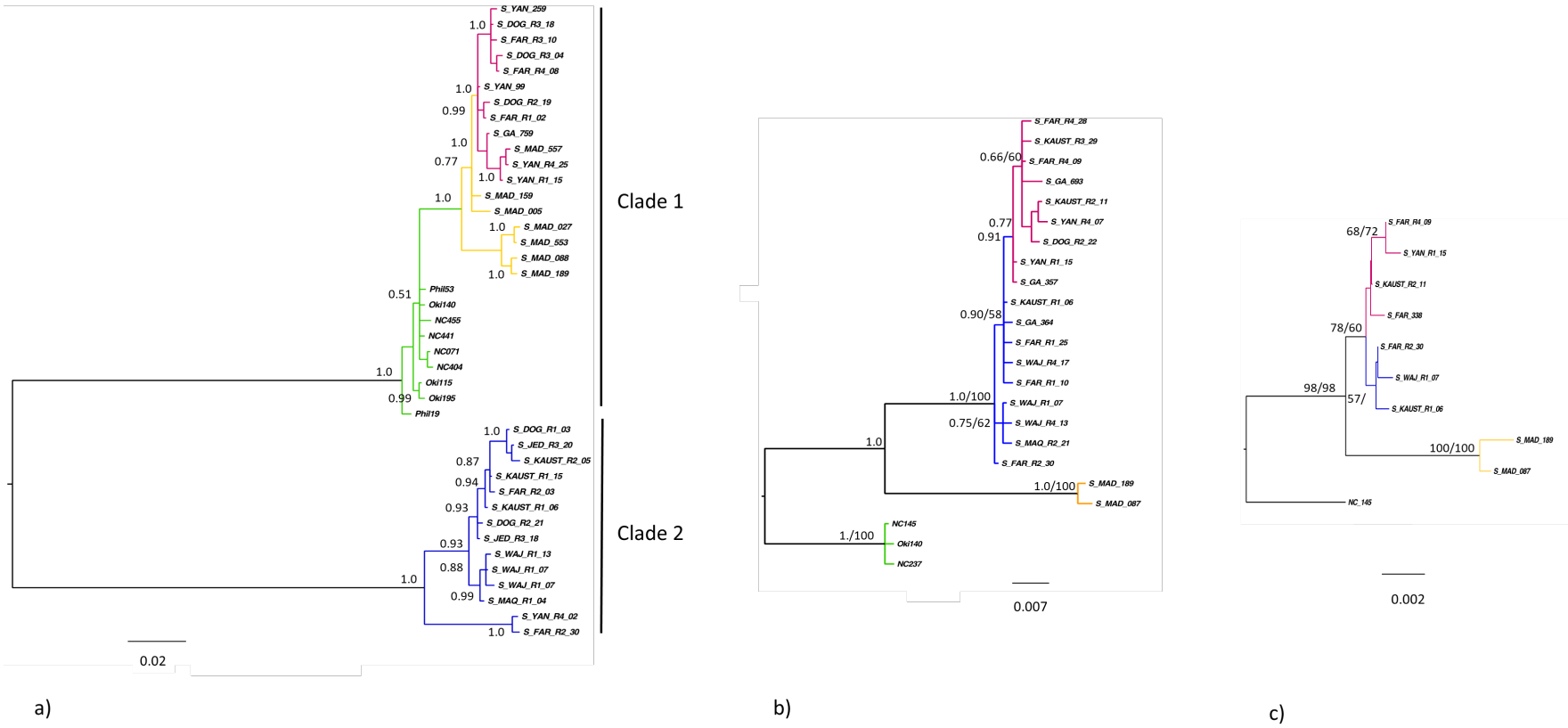

Mitochondrial phylogenies of the genus *Stylophora*. a). Bayesian tree of the *atp6*-mt*ORF* locus. b). Bayesian tree for the CR gene and c). Maximum Likelihood (ML) tree for the 12S gene. Node support are given in Bayesian Probabilities (BPP) for the mt*ORF*, BPP/ML for the mtCR and ML/NJ for the 12S. Colors are as follow: Red: Haplotypes from Arabian Gulf, Red Sea and Gulf of Aden placed in Clade 1 (*RS_LinA*). Yellow: haplotypes from Madagascar. Green: haplotypes from Indo-Pacific (Philippines, Okinawa, New Caledonia) and Blue: Red Sea and Gulf of Aden haplotypes placed in Clade 2 (*RS_LinB).* Haplotypes names are given in agreement to the region where the haplotype was found in higher frequency (MAQ=MAQNA, WAJ=ALWAJH, YAN=YANBU, KAUST = KAUST, JEDDAH=JED, DOG = DOGA, FARASAN = FAR).

Figure 3.

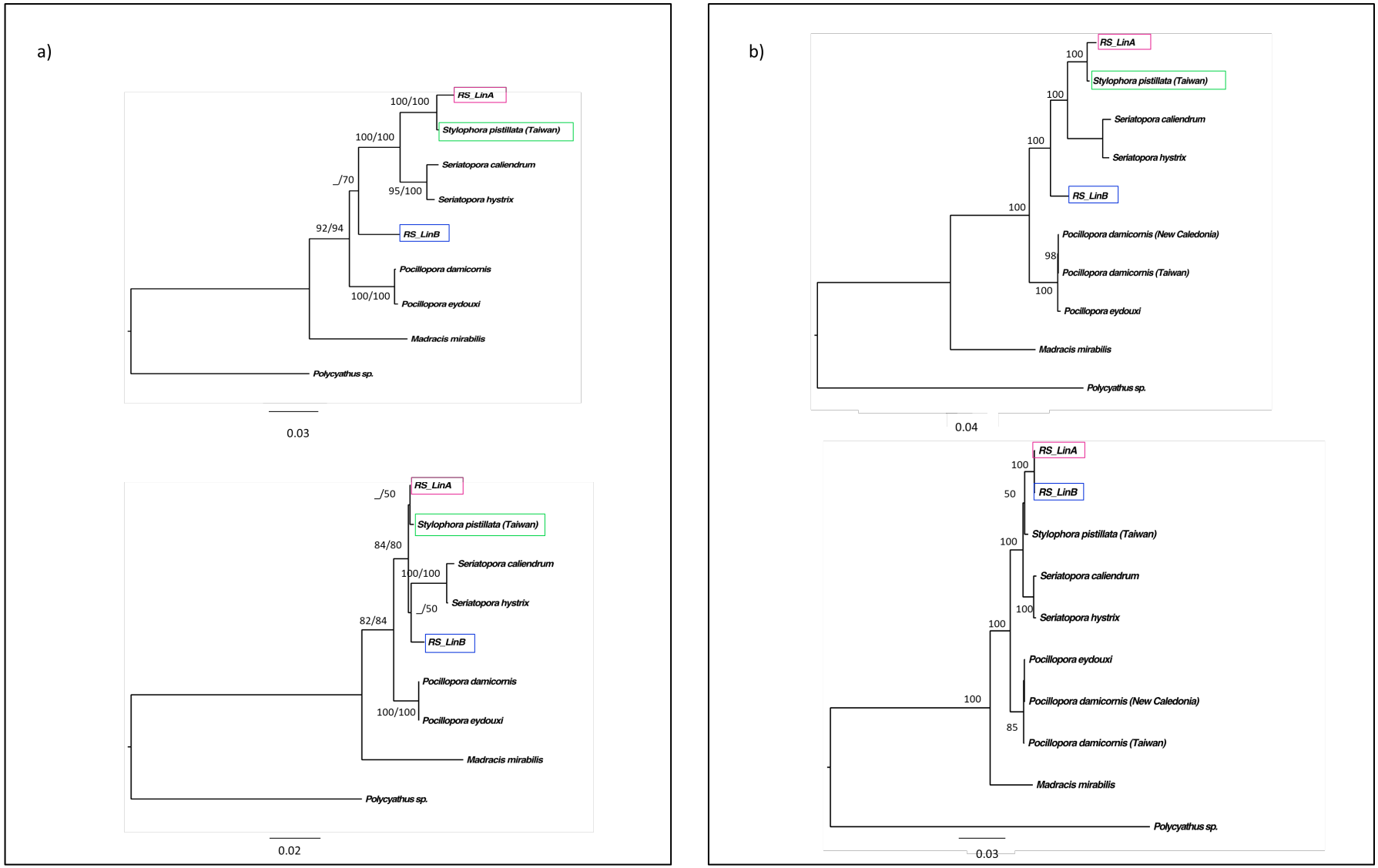

Mitochondrial phylogenies of the family Pocilloporidae and recombination analyses. a) Position of the *RS_LinA* and *RS_LinB* in a family phylogeny of the full *atp6* (above) and *nd6* genes (below). b). ML phylogenies from the recombination hypotheses: phylogeny derived from the recombinant region –minor parent–, including the *nd6*, *atp6*, and *mtORF* genes; 2415bp (above) and phylogeny from mtDNA genes outside the recombinant region –from the major parent – 9555bp (below).

Figure 4.

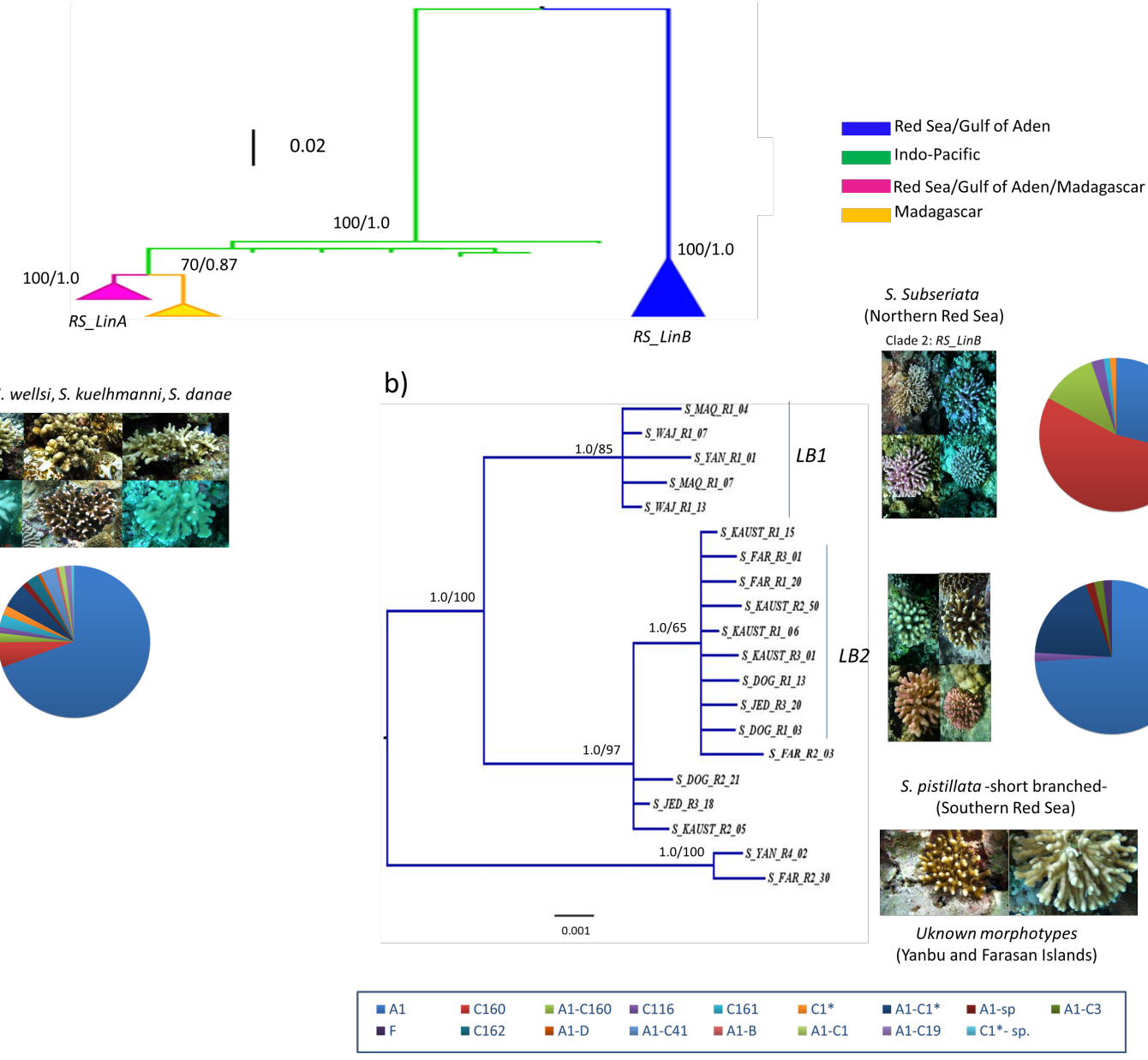

Extended *atp6*-mt*ORF* phylogenies for a). *RS_LinA* and b). *RS_LinB.* Morphotypes and *Symbiodinium* types associated with each lineage are shown.

Figure 5.

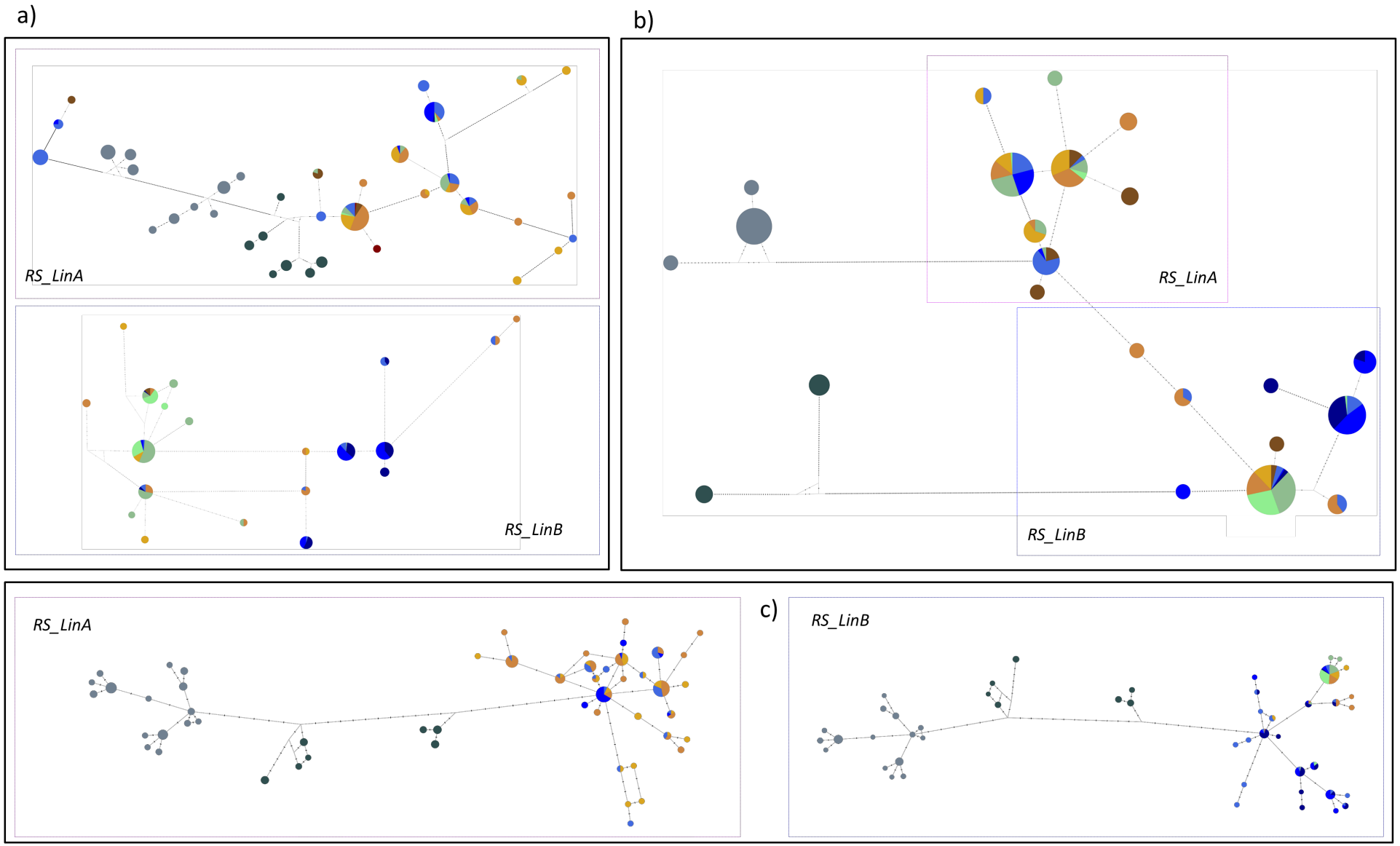

Network trees. a). *atp6*-mt*ORF* b). Control Region (CR) c). *hsp70.* Mutations are indicated as vertical lines.

Supplementary Figure *S1.*

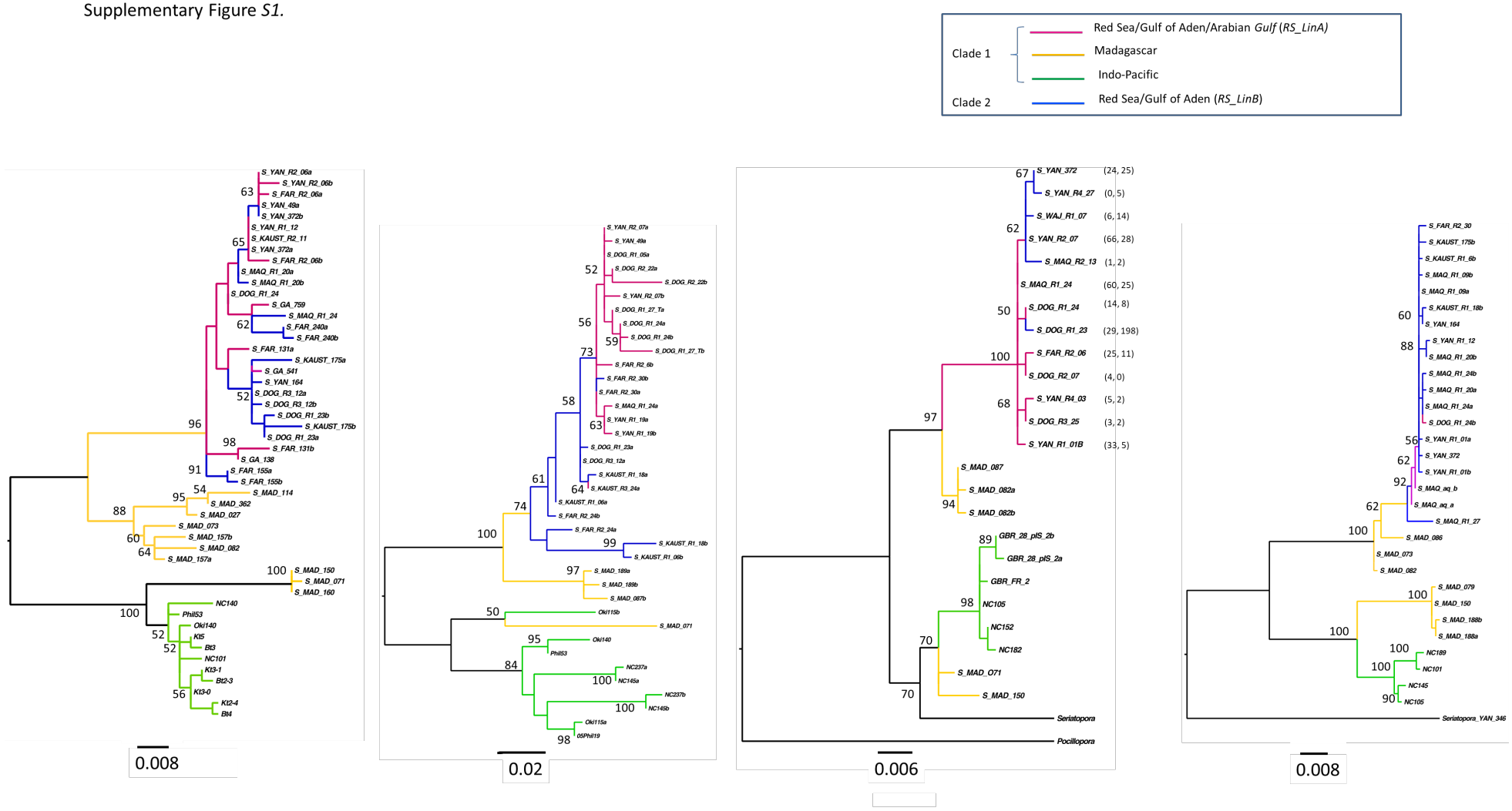

Nuclear phylogenies of the genus *Stylophora*. a). ITS1 b). ITS2 c). *hsp70* d). *PMCA*. Colors and haplotypes names are in agreement with those in the *atp6*-mt*ORF* phylogenies (see legend in Figure 2). In the *hsp70* phylogeny, the number of specimens found per haplotype in each lineage are placed within parentheses (*RS_LinA*, *RS_linB).*

Supplementary Figure *S2a*.

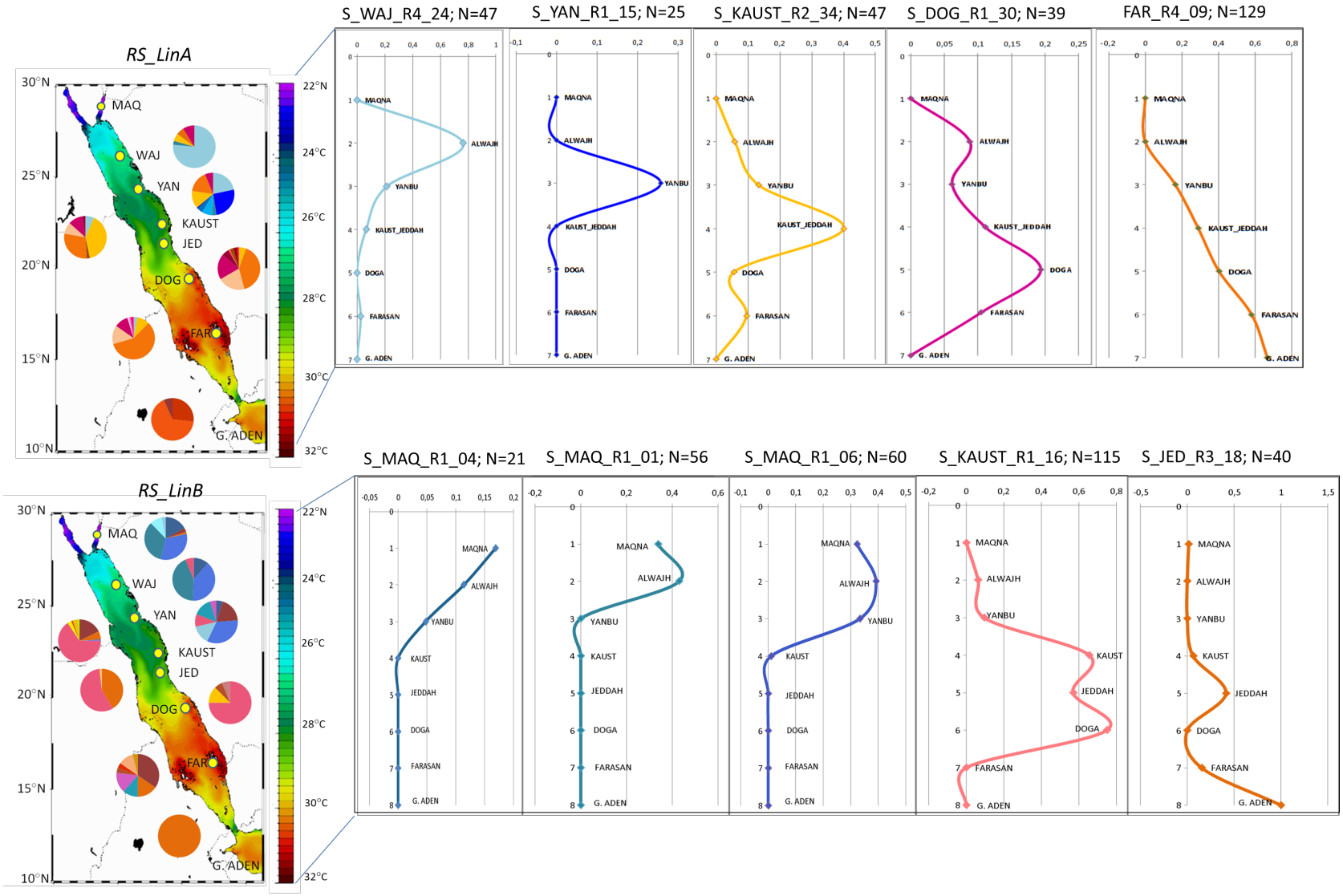

Distribution of haplotype frequencies along the gradient as per mtDNA lineage (*atp6*-mt*ORF* locus). Frequencies are indicated for the most common haplotypes. Axis x=relative frequencies.

Supplementary Figure *S2b*.

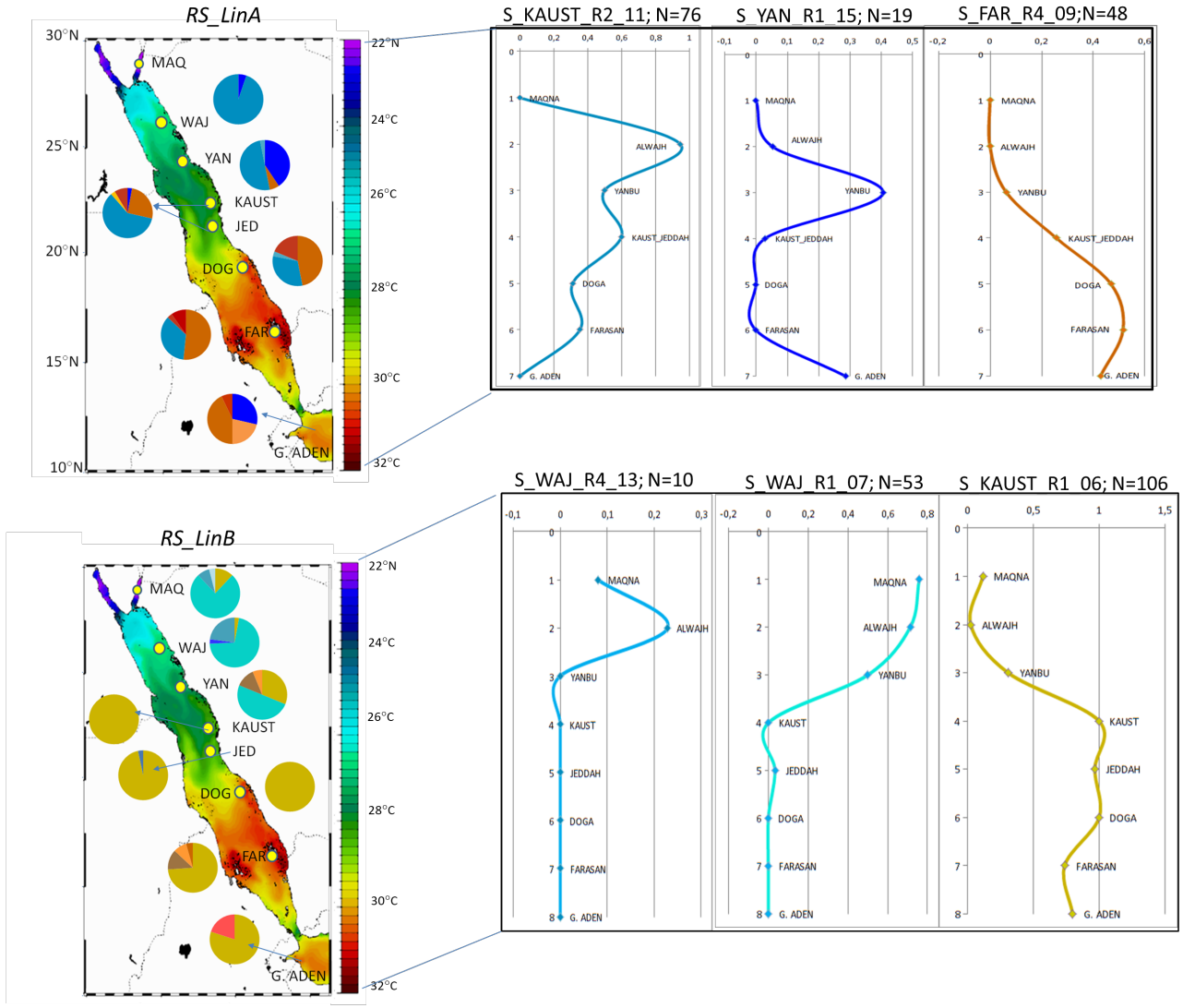

Distribution of haplotype frequencies along the gradient as per mtDNA lineage (CR fragment). Frequencies are indicated for the most common haplotypes. Axis x=relative frequencies.

Supplementary Figure *S2c.*

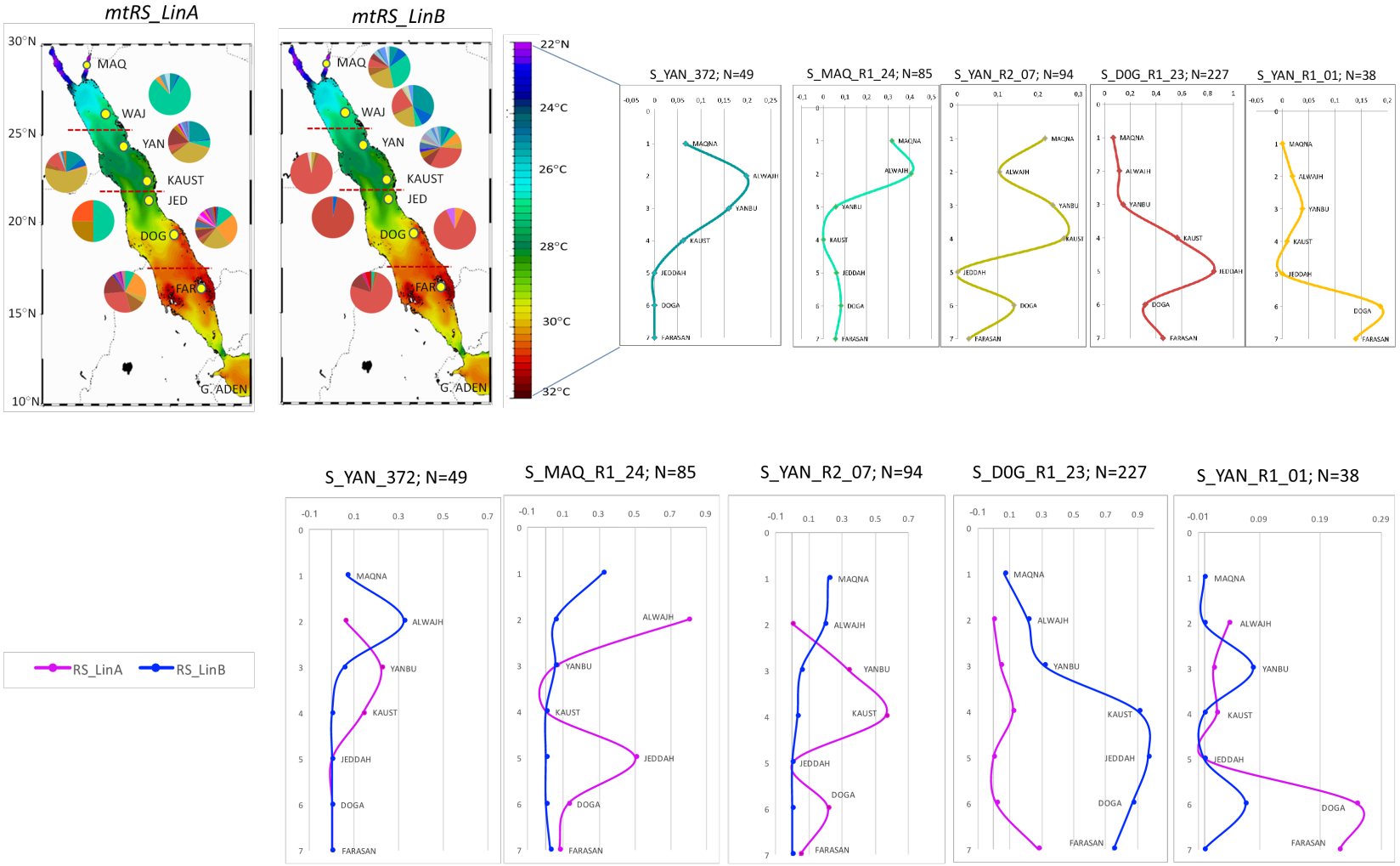

Distribution of haplotype frequencies along the gradient (*hsp70* fragment). Haplotype frequencies of the most common haplotypes (above) and in agreement with mtDNA lineages (below). Axis x=relative frequencies.

Supplementary Figure *S3*.

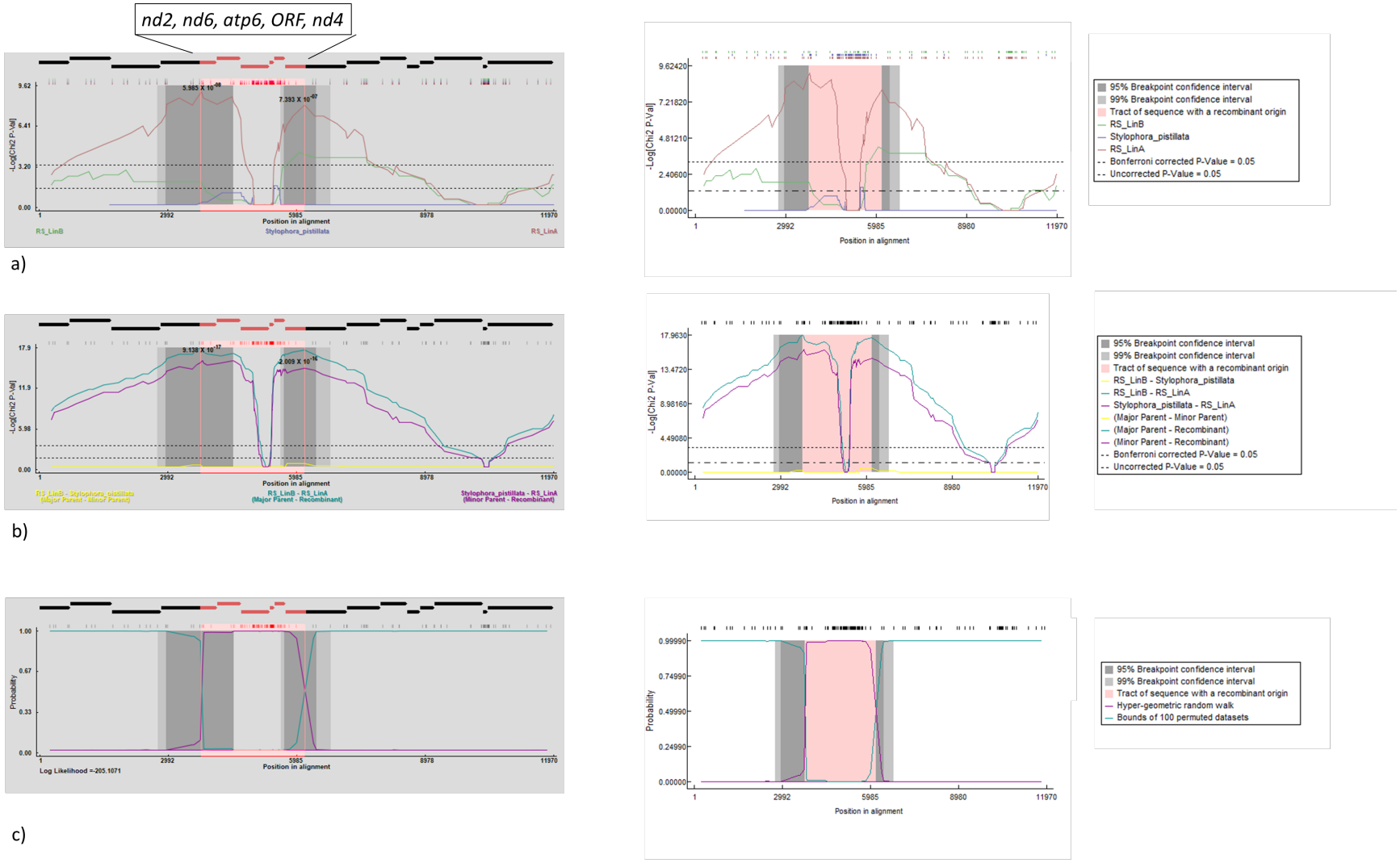

Recombination analyses. Identification of recombinant sequences and estimation of break points by different recombination methods. a). CHIMAERA b). MAXCHI and c) BURT.